RM E58E21

NACA

RESEARCH MEMORANDUM

COMBUSTOR PERFORMANCE WITH VARIOUS HYDROGEN-OXYGEN INJECTION METHODS IN A 200-POUND-THRUST ROCKET ENGINE

By M. F. Heidmann and Louis Baker, Jr.

Lewis Flight Propulsion Laboratory
Cleveland, Ohio

NATIONAL ADVISORY COMMITTEE
FOR AERONAUTICS

WASHINGTON
September 30, 1958

NACA RM E58E21

NATIONAL ADVISORY COMMITTEE FOR AERONAUTICS

RESEARCH MEMORANDUM

COMBUSTOR PERFORMANCE WITH VARIOUS HYDROGEN-OXYGEN INJECTION METHODS IN A 200-POUND-THRUST ROCKET ENGINE

By M. F. Heidmann and Louis Baker, Jr.

SUMMARY

Characteristic velocity of liquid oxygen and gaseous hydrogen was determined as a function of mixture ratio in a nominal 200-pound-thrust variable-length rocket engine. Fourteen different injectors, which varied mixing and oxygen atomization, were evaluated. The heat-transfer rates were determined for seven of these injectors. Injector designs included (1) triplets of two hydrogen jets impinging on one oxygen jet with variations in impingement angle and orifice size, (2) concentric injection with hydrogen surrounding a jet of oxygen, (3) radial injection of oxygen with variations in hydrogen injection, and (4) oxygen atomization by two impinging jets with variations in hydrogen injection. The triplet and concentric arrangements were studied in both single and multiple units.

The degree of oxygen atomization appeared to be the primary factor affecting efficiency in agreement with a vaporization model of combustion. Increasing the oxygen-jet size generally produced a reduction in characteristic exhaust-velocity efficiency regardless of the atomization method.

A decrease in efficiency with an increase in mixture ratio was encountered with several injectors. This implies incomplete mixing for a combustion process limited by physical processes. The effect was most pronounced with large spacing between oxygen-injection orifices or poor dispersion from a single orifice. Hydrogen-injection changes also contributed to performance variations with mixture ratio. The method of hydrogen injection appeared to affect both oxygen atomization and dispersion.

Heat rejection showed no significant variation with injection method. Maximum heat-rejection rates of 3.5 to 4 Btu per second per square inch occurred near the stoichiometric mixture ratio.

INTRODUCTION

High combustion efficiency with a minimum of complexity is continually sought in the design of injectors for rocket engines. Realization of this goal depends on a better understanding of the effects of design on performance. In order to gain a greater insight into the effect of injector configuration on the combustion characteristics of the hydrogen-oxygen system, 14 injectors were studied in a 200-pound-thrust rocket engine. The configurations included triplet, concentric-tube, radial-jet, and self-impinging jet injectors. Some of these configurations were studied because they pertained to the design of a hydrogen-cooled injector for a larger thrust engine.

A previous study using similar apparatus (ref. 1) showed qualitatively that combustor efficiency depends more on oxygen atomization than on hydrogen dispersion or propellant mixing. The present study may be considered an extension of this work in that a more quantitative evaluation was made of the effect of these parameters on combustor performance.

The characteristic exhaust velocity (C^*) was measured for all the injectors over a range of mixture ratios. In some instances chamber-length variations were used to evaluate performance more accurately. Heat-transfer measurements were also made for seven of the injectors. Stability characteristics were studied separately and are reported in reference 2. Gaseous hydrogen at room temperature rather than liquid hydrogen was used for all tests because it more nearly simulated entrance conditions for a regeneratively cooled rocket engine.

INJECTORS

Triplet

Six triplet injectors with two hydrogen jets impinging on one oxygen jet, as shown in figure 1(a), were studied. These included four injectors with a single element, one with four elements, and one with nine elements. Orifice diameters of the single- and four-element injectors were equal. The diameters of the orifices in the nine-element injector were about one-half as large. Hydrogen-injection velocity, tabulated in figure 1, is the calculated velocity for isentropic flow assuming a total flow of 0.12 pound per second and a chamber pressure of 300 pounds per square inch.

Concentric Tube

Two concentric-tube injectors (fig. 1(b)) with an oxygen jet surrounded by a hydrogen annulus were used. These were a single- and a nine-element injector. The oxygen orifice diameter of the nine-element injector was about one-third that of the single-element injector.

Radial Jet

Two injectors with radial injection of eight oxygen jets (fig. 1(c)) were used. Hydrogen was injected from 10 centrally located orifices in one injector and from 45 distributed holes in the other.

Impinging Jet

Four injectors with oxygen injected as two impinging jets were used as shown in figure 1(d). Hydrogen-orifice arrangements varied as follows: (1) 45 distributed holes, (2) 16 peripheral holes, (3) 10 center holes, and (4) one center hole. Hydrogen injection velocity differed for these arrangements by a factor of about 3.

APPARATUS AND PROCEDURE

Test Facilities

Small-scale test facilities similar to those described in references 1 and 3 were used. Hydrogen, at approximately ambient temperature, was delivered to the rocket engine from high-pressure storage cylinders after one stage of pressure regulation. The flow rate, which was limited to a total flow of about 0.12 pound per second, was measured with a Venturi meter. Liquid oxygen at 140° R was supplied from a pressurized tank immersed in liquid nitrogen. Two rotary-vane-type flow meters were used to indicate oxygen flow rate. Chamber pressure was determined from the average indication of two strain-gage pressure transducers.

The combustor consisted of an injector, uncooled cylindrical chamber, and water-cooled convergent nozzle in separable units. A chamber diameter of 2 inches and a nozzle throat diameter of 0.750 inch (contraction ratio of 7.0) were used in all of the tests.

Heat-transfer rates were measured in a 2-inch long, water-cooled chamber segment adjacent to the exhaust nozzle, shown in figure 2.

Water-air spray photographs were obtained for all the injectors to show qualitatively their atomization and dispersion characteristics. The mean operating mass flow rates were simulated. This approximated jet velocity and momentum for both oxygen and hydrogen except in the region where airflow was greater than critical.

Performance Evaluation

Engine firings from 3- to 5-seconds duration, sufficient to establish steady-state operation, were used. A series of oxidant-fuel mixture ratios was run for each of several hydrogen flow rates. In this manner a mixture-ratio range of about 2 to 10 and total flow rates of about 0.4 to 0.8 pound per second were covered. Chamber lengths (cylindrical sections) from 3 to 24 inches were used. The range of operating conditions and chamber lengths differed somewhat for the various injectors.

The characteristic exhaust velocity C^* and mixture ratio o/f were evaluated for each test condition. Experimental values, expressed as C^* efficiency, are percentages of the theoretical values shown in figure 3.

Total heat transfer during a finite time interval was reduced to heat-transfer rate per unit area. The reported values were normalized to 300 pounds per square inch absolute chamber pressure by assuming direct proportionality between the heat-transfer rate and the pressure.

RESULTS AND DISCUSSION

The experimental performance values obtained with the 14 injectors are presented in table I. Performance curves, water-air spray photographs, and injector designs are shown for each injector in figures 4 to 7.

General Observations

The C^* (characteristic exhaust velocity) efficiency was generally greater than 70 percent for all injectors. As observed in reference 1 the efficiency is higher than that obtained with heptane-oxygen combination for similar injection methods (ref. 3). The result agrees with the hypothesis that propellant vaporization is a controlling process in liquid-propellant combustors. Analytical studies based on this hypothesis (ref. 4) have shown that for a given chamber length the heptane vaporization rate is about one-third that for liquid oxygen for the same initial drop size distributions.

Injectors with 0.04- to 0.047-inch-diameter oxygen orifices gave the best performance. These included the nine-element triplet, nine-element concentric-tube, and radial-jet injectors. Of these, the triplet gave the highest performance. The C^* efficiency exceeded 95 percent in a 12-inch chamber length and remained above 90 percent in a 3-inch chamber length. The performance with injectors having larger oxygen orifices was generally lower. The result attests to the importance of oxygen atomization.

The performance with several injectors depended on hydrogen distribution and injection velocity. This effect was shown in the impinging oxygen-jet injector where changes in the size and orientation of the hydrogen jet caused 15-percent changes in C^* efficiency.

Several of the injectors showed a pronounced decrease in C^* efficiency with an increase in mixture ratio o/f. This characteristic will be subsequently discussed in the performance analysis of individual injectors.

High-frequency combustion instability was observed during some test conditions. This condition primarily occurred with high-efficiency performance. These stability characteristics were studied separately and are reported in reference 2.

Combustion Model

A combustion model proved useful in previous experimental studies (refs. 4 to 8) assumed propellant vaporization as the rate-controlling step in the combustion process. Reference 8 is particularly applicable to this study. It shows that the shape of the curve of characteristic exhaust velocity against oxidant-fuel ratio indicates whether the oxidant or fuel is completely vaporized. If some constant fraction of the oxidant is not vaporized, the C^* efficiency is relatively constant with changes in o/f. A constant fraction of unvaporized fuel gives a pronounced decrease in efficiency with an increase in o/f.

This analysis was extended to the case of gaseous hydrogen and liquid oxygen. The assumptions used differed from those of reference 8 in the following manner: Hydrogen was assumed incompletely mixed rather than incompletely vaporized, and this unused hydrogen was assumed to have a finite volume rather than a negligible volume. The C^* variations with o/f obtained with these assumptions (fig. 8) are similar to those of reference 8, that is, a constant fraction of unmixed hydrogen in the exhaust causes a decrease in C^* efficiency with o/f, whereas a constant fraction of oxygen escaping unvaporized causes a constant or gradually increasing efficiency with o/f. These performance trends will aid in interpreting the experimental data.

Performance Analysis of Characteristic Exhaust Velocity

Triplet injector. - The C^* performance obtained in a 12-inch chamber with the triplet injectors is summarized in figure 9(a). With single elements the performance level was nearly identical for 20° and 40° impingement angles. This represents about a 20-percent increase over nonimpinging streams. The spray photographs (fig. 4) show a comparable change in that the improvement in atomization and dispersion is more pronounced for an impingement-angle change of 0° to 20° than for a change of 20° to 40°. The higher C^* efficiency observed with the nine-element injector than for the four-element injector may also be attributed to better spray properties. Increasing the number of orifices and decreasing the diameter of the orifices should improve atomization and dispersion of oxygen.

All the single-element injectors show a decrease in C^* efficiency with an increase in oxidant-fuel ratio. This implies incomplete propellant mixing. With single elements the liquid oxygen is concentrated along the chamber axis and hydrogen is dispersed over a 1-inch radial distance from this axis. Mixing processes, therefore, must take place over a lateral distance of 1 inch for complete mixing. Therefore, improved mixing would be expected from a decrease in this lateral mixing distance. The four-element injector is an example of such a change. In this case, four elements identical to the single element were used in the 2-inch-diameter chamber. The lateral mixing distance was reduced considerably; the gradual rise in C^* efficiency with o/f obtained experimentally is evidence of a marked increase in mixing.

The performance obtained with the offcenter single-element injector is another example of a change in lateral mixing distance. The effective mixing distance is larger than that of an equivalent central element. The decrease in efficiency obtained may be attributed to poor mixing.

An example of a change in mixing with chamber length is shown by the nine-element-injector performance in figures 4(d) and (e). As chamber length is reduced, injector performance develops a trend of decreasing C^* efficiency with o/f which indicates less complete mixing in short chambers.

A decrease in C^* efficiency with o/f was also observed in reference 1. This primarily occurred when one instead of two oxygen orifices were used. The larger lateral mixing distance with single orifice would account for this performance trend.

Analyzing the data in this manner shows that lateral mixing in some instances is a rate-limiting process in combustion. Generalizing the results for triplets shows that the chamber length at which mixing is complete varies with spacing between oxygen orifices. Interpolation of

the experimental data shows that complete mixing is obtained in a length of 8 inches with 3/8-inch spacing, 13 inches with 0.7-inch spacing, and considerably more than 12 inches for a single element representing a 2-inch spacing. As a rough rule-of-thumb, therefore, chamber length must be about 20 times larger than the spacing between oxygen orifices in order to assure complete mixing.

Concentric-tube injector. - The performance of the concentric-tube injectors is summarized in figure 9(b). Qualitatively the performance is similar to that obtained with triplet injectors for equivalent size oxygen orifices. Single-element performance again decreases rapidly with an increase in o/f indicating incomplete mixing. The poorer dispersion with the single-element injector than with the nine-element injector is shown by the spray photographs in figure 5 and suggests inefficiency caused by incomplete lateral mixing. Therefore, for concentric-tube injectors dispersion of the oxygen as well as atomization is required for high performance.

Radial-jet injector. - The performance obtained with radial oxygen jets is summarized in figure 9(c). Hydrogen was concentrated near the chamber axis with one injector and uniformly distributed with the other. By adjusting for the differences in chamber lengths used the C^* efficiency was about the same for both injectors in the high o/f region, but centrally injected hydrogen was definitely better in the low o/f region. Apparently, oxygen atomization differed in this region. With central injection the hydrogen jets were of higher velocity and orientated for a greater exchange of momentum with the oxygen than with distributed injection. As a result, oxygen atomization was improved as shown by the photographs in figure 6. This difference apparently affected performance only when a high proportion of hydrogen to oxygen existed (low o/f region).

Impinging oxygen-jet injector. - The performance of the impinging oxygen-jet injectors in which hydrogen was injected in various orientations is summarized in figure 9(d).

Injecting hydrogen through a 45-hole plate gave a C^* efficiency of 88 percent with no significant change with o/f. On the basis of the combustion model, incomplete oxygen vaporization is implied with full utilization of the hydrogen. This injector introduced the hydrogen uniformly and at a low velocity. The spray photographs (figs. 7(a) and (b)) show no effect of hydrogen flow on the atomization process. This C^* performance, therefore, will be used as a reference condition in evaluating the effect of changes in hydrogen injection.

The C^* efficiency level was less than 85 percent with hydrogen injected from 16 peripheral holes. Such a hole arrangement suggests poorly mixed propellants. The rising C^* efficiency with o/f, however, implies incomplete oxygen vaporization rather than incomplete mixing. The efficiency level is also lower than with the 45-hole plate indicating less complete oxygen vaporization. Corresponding changes in oxgyen atomization are not evident in the spray photographs of figures 7(a) to (d); however, conditions may differ considerably within the combustor.

Incomplete mixing is implied by the performance curve obtained with hydrogen injected centrally from 10 holes. The high performance level, however, also indicates improved oxygen atomization. The spray photographs (figs. 7(e) and (f)) show that oxygen atomization is affected by hydrogen flow and that oxygen is directed away from the axis of the chamber which may contribute to poor mixing.

Hydrogen injected from a single center hole gave an increase in C^* efficiency with an increase in o/f. The spray photographs (figs. 7(g) and (h)) again show that oxygen atomization is affected by hydrogen flow. This effect presumably varies with o/f. The over-all effect on C^* efficiency is not clear, however, because changes in drop size, drop acceleration, and oxygen dispersion would occur simultaneously with changes in o/f. At low o/f values, such interaction apparently causes performance losses.

Heat Transfer

The heat-transfer data are summarized in figure 10. The rates reported are the average values for a 2-inch chamber segment installed near the exhaust nozzle. Heat-transfer rates were usually of the order of 3 to 4 Btu per second per square inch. The maximum rate was obtained near the stoichiometric oxidant-fuel ratio of 8. The higher performance injectors generally gave the highest heat-injection rates. The results deviate from this trend in the low mixture ratio region, and the distinction between injectors is less evident. A heat-transfer rate of 3.08 Btu per second per square inch at an o/f of 3.2 was computed theoretically for this engine configuration. A gas-side wall temperature of 450° F and gas-film properties at 2300° F were assumed for these calculations. Experimental rates at this o/f are within 10 percent of this value.

A greater differentiation between injectors would be expected for average values for the entire chamber length. Measurements for different chamber lengths were obtained for several injectors. The C^* efficiency changes with length, however, were small and did not significantly affect heat transfer at the measuring station.

A heat-transfer rate from 3 to 4 Btu per second per square inch results in a loss in performance of about 1 percent per 6 inches of chamber length. The C^* efficiencies have not been corrected for these losses. The corrections become significant when performance changes with chamber length are analyzed.

SUMMARY OF RESULTS

A study of propellant atomization and distribution with 14 different injectors using liquid oxygen and gaseous hydrogen has shown that C^* performance primarily depends on the effectiveness of oxygen atomization. Injecting oxygen by a 0.040-inch-diameter jet gave a C^* efficiency of about 90 percent in a 3-inch chamber length. Increasing the oxygen-jet size generally gave a reduction in efficiency regardless of the injection method.

Variations in design of specific injection methods gave the following results.

(1) Triplet: Single-element performance increased with impingement angle up to an included angle of 20°. Multiple elements showed less variations in C^* efficiency with o/f than single elements. Element spacing or oxygen dispersion appeared important in these variations implying that lateral mixing limits the combustion-rate process.

(2) Concentric tube: Performance level was comparable with that obtained with triplet injectors.

(3) Radial jet: An orientation of hydrogen and oxygen jets to give maximum interchange of momentum gave the highest C^* efficiency.

(4) Impinging jet: Variations in hydrogen distribution and injection velocity affected both C^* efficiency level and variations in efficiency with o/f. Compared with the condition of uniformly distributed hydrogen at low injection velocity, the interaction between hydrogen jets and oxygen sprays in some instances caused performance losses.

Lewis Flight Propulsion Laboratory
National Advisory Committee for Aeronautics
Cleveland, Ohio, July 14, 1958

REFERENCES

1. Auble, Carmon M.: A Study of Injection Processes for Liquid Oxygen and Gaseous Hydrogen in a 200-Pound-Thrust Rocket Engine. NACA RM E56I25a, 1957.

2. Baker, Louis, Jr., and Steffen, Fred W.: Screaming Tendency of the Gaseous Hydrogen - Liquid Oxygen Propellant Combination. NACA RM E58E09, 1958.

3. Heidmann, M. F., and Auble, C. M.: Injection Principles from Combustion Studies in a 200-Pound-Thrust Rocket Engine Using Liquid Oxygen and Heptane. NACA RM E55C22, 1955.

4. Priem, Richard J.: Propellant Vaporization as a Criterion for Rocket Engine Design; Calculations of Chamber Length to Vaporize Various Propellants. NACA TN 3883, 1958.

5. Priem, Richard J.: Propellant Vaporization as a Criterion for Rocket-Engine Design; Calculations of Chamber Length to Vaporize a Single n-Heptane Drop. NACA TN 3985, 1957.

6. Priem, Richard J.: Propellant Vaporization as a Criterion for Rocket-Engine Design; Calculations Using Various Log-Probability Distributions of Heptane Drops. NACA TN 4098, 1957.

7. Heidmann, M. F.: Propellant Vaporization as a Criterion for Rocket-Engine Design; Experimental Effect of Fuel Temperature on Liquid-Oxygen - Heptane Performance. NACA RM E57E03, 1957.

8. Heidmann, Marcus F., and Priem, Richard J.: Propellant Vaporization as a Criterion for Rocket-Engine Design; Relation Between Percentage of Propellant Vaporized and Engine Performance. NACA TN 4219, 1958.

TABLE I. - SUMMARY OF EXPERIMENTAL INJECTOR PERFORMANCE

(a) Triplet injector

[One axial liquid-oxygen jet, two impinging hydrogen jets per element.]

Run	Chamber length, in.	Impingement angle, deg	Fuel weight flow, lb/sec	Fuel-injection velocity, ft/sec	Oxidant weight flow, lb/sec	Total weight flow, lb/sec	Chamber pressure, lb/sq in. abs	Oxidant-fuel weight ratio	Characteristic exhaust velocity, C*, ft/sec	Percent of theoretical C*	Heat-transfer rate, Btu/(sec)(sq in.)
Single element; oxygen flow area, 0.0075; hydrogen flow area, 0.0433											
142	12	[a]0	0.093	3120	0.431	0.524	249	4.65	6738	85.9	
143			.091	2838	.542	.633	274	5.93	6139	81.7	
144			.090	2735	.624	.714	283	6.90	5621	77.4	
145			.090	3370	.308	.398	219	3.40	7842	98.0	
120			.074	2872	.426	.500	219	5.73	6230	82.3	
147			.065	2640	.491	.556	213	7.58	5432	76.7	
146			.064	2820	.361	.425	194	5.64	6473	85.3	
119			.060	2790	.379	.439	184	6.36	5960	80.5	
117			.043	2337	.422	.465	162	9.82	4950	74.5	
118			.036	2218	.430	.466	144	11.88	4390	71.5	
129		20	.051	2370	.362	.413	189	7.10	6507	90.2	
130			.050	2350	.366	.416	187	7.30	6392	89.3	
128			.036	2052	.423	.459	157	11.92	4863	79.2	
126		40	.056	2309	.422	.478	214	7.54	6370	89.6	
124			.049	2190	.455	.504	199	9.38	5610	84.5	
122			.042	2240	.393	.435	166	9.42	5430	81.8	
125			.041	2027	.468	.509	181	11.56	5060	81.5	
295		[b]20	.126	Sonic	.342	.468	233	2.71	7190	90.1	2.78
283			.097	3205	.386	.483	252	3.96	7455	93.7	3.75
284			.094	2525	.611	.705	324	6.48	6568	89.1	3.37
293			.089	3300	.368	.457	223	4.14	7047	88.9	3.40
296			.082	3185	.361	.443	215	4.42	7008	88.8	2.62
294			.060	2600	.404	.464	200	6.73	6223	85.1	2.70
297			.053	2657	.274	.327	154	5.21	6800	88.3	1.73
Four elements; oxygen flow area, 0.0302; hydrogen flow area, 0.1731											
178	12	40	0.123	915	0.501	0.624	313	4.07	7165	90.2	3.61
177			.123	620	.693	.816	396	5.64	6935	91.3	4.40
176			.122	860	.544	.666	330	4.44	7081	89.8	2.73
183			.120	1048	.412	.532	266	3.45	7145	89.3	2.72
184			.082	640	.571	.653	295	6.98	6355	87.7	3.06
185			.080	542	.703	.783	344	8.75	6279	92.4	3.16
186			.078	485	.809	.887	373	10.38	6008	93.4	3.35
Nine elements; oxygen flow area, 0.0113; hydrogen flow area, 0.0951											
241	3	30	0.113	1425	0.533	0.646	330	4.71	7356	94.0	-----
242			.090	1480	.398	.488	252	4.44	7436	94.4	-----
243			.074	1080	.572	.646	288	7.69	6419	90.9	-----
244			.062	1130	.437	.499	231	7.09	6666	92.4	-----
245			.050	979	.461	.511	216	9.15	6087	90.8	-----
237	6		.129	1690	.468	.597	315	3.64	7597	95.1	4.08
236			.128	1530	.529	.657	346	4.12	7583	95.5	5.36
238			.127	1920	.389	.516	271	3.06	7563	94.4	3.71
226			.127	1910	.387	.514	273	3.05	7648	95.5	3.05
227			.124	1710	.454	.578	298	3.66	7425	92.9	3.00
239			.085	1155	.579	.664	308	6.83	6679	91.7	4.58
231			.082	1090	.584	.666	316	7.10	6833	94.8	-----
240			.081	1320	.419	.500	255	5.16	7344	95.2	3.88
229			.081	1390	.384	.465	242	4.76	7494	95.9	2.69
224			.062	1075	.470	.532	243	7.53	6578	92.6	3.23
232			.061	1130	.421	.482	227	6.92	6781	93.4	-----
233			.060	1003	.525	.585	253	8.81	6228	91.8	-----
234			.060	960	.571	.631	266	9.58	6071	91.9	-----
235			.058	870	.639	.697	281	11.06	5806	92.2	-----
225			.051	958	.483	.534	225	9.45	6067	91.4	3.08
193	12		.123	1640	.446	.569	310	3.61	7742	96.9	3.49
192			.123	1850	.383	.506	273	3.11	7666	95.7	2.76
194			.123	1533	.504	.627	333	4.09	7547	95.1	3.89
199			.123	1655	.451	.574	307	3.66	7600	95.2	3.88
190			.123	2155	.322	.445	231	2.62	7376	92.5	2.26
191			.122	1875	.383	.505	267	3.15	7513	93.8	2.09
200			.118	1450	.510	.628	336	4.32	7602	96.2	4.44
201			.097	1210	.563	.660	335	5.83	7213	95.7	4.26
196			.083	1070	.577	.660	326	6.92	7018	96.7	4.04
198			.074	970	.590	.664	313	8.02	6698	96.0	4.10
197			.073	1020	.596	.669	302	8.16	6414	92.4	3.09

TABLE I. - Continued. SUMMARY OF EXPERIMENTAL INJECTOR PERFORMANCE

(b) Concentric-tube injector

Run	Chamber length, in.	Fuel weight flow, lb/sec	Fuel-injection velocity, ft/sec	Oxidant weight flow, lb/sec	Total weight flow, lb/sec	Chamber pressure, lb/sq in. abs	Oxidant-fuel weight ratio	Characteristic exhaust velocity, C*, ft/sec	Percent of theoretical C*	Heat-transfer rate, Btu/(sec)(sq in.)
Single element; oxygen flow area, 0.0108; hydrogen flow area, 0.0490										
6	8	0.1238	3465	0.456	0.5800	256	3.68	6683	83.7	----
5		.1228	Sonic	.312	.4350	212	2.54	7379	92.8	----
7		.1228	3360	.607	.7300	265	4.94	5496	70.7	----
14		.1200	3555	.415	.5350	240	3.46	6780	84.8	----
15		.1200	3065	.660	.7800	290	5.50	5630	73.8	----
8		.1114	3140	.757	.8680	265	6.80	4622	63.6	----
18	14	.1210	3635	.324	.4450	235	2.68	7339	92.0	----
20		.1210	3200	.368	.4890	277	3.04	7873	98.3	----
21		.1160	2845	.444	.5600	307	3.83	7619	95.6	----
23		.1160	2580	.602	.7180	344	5.19	6660	86.4	----
22		.0969	2475	.583	.6799	302	6.02	6174	82.4	----
26		.0844	2450	.529	.6134	266	6.27	6026	81.1	----
24		.0831	2320	.672	.7551	279	8.09	5135	73.8	----
25		.0829	2360	.611	.6939	273	7.37	5466	76.5	----
30	22	.1280	2970	.439	.5670	321	3.43	7870	98.4	----
31		.1230	2605	.517	.6400	357	4.20	7754	97.8	----
33		.1210	2455	.572	.6930	380	4.73	7622	97.5	----
35		.0843	2460	.405	.4893	264	4.80	7500	96.2	----
36		.0831	2190	.494	.5771	297	5.94	7152	95.2	----
37		.0821	2050	.582	.6641	314	7.09	6570	91.1	----
38		.0801	1965	.661	.7411	322	8.25	6039	87.3	----
Nine elements; oxygen flow area, 0.0113; hydrogen flow area, 0.0939										
246	3	0.123	1890	0.375	0.498	270	3.04	7808	97.5	----
247		.123	1600	.478	.601	320	3.87	7667	96.2	----
248		.123	1450	.581	.704	356	4.72	7282	93.1	----
250		.082	1100	.665	.747	316	8.16	6091	87.8	----
249		.081	1300	.459	.540	263	5.68	7026	92.7	----
204	12	.122	1535	.512	.634	333	4.21	7483	94.2	3.55
203		.121	1780	.379	.500	284	3.13	8071	100.8	3.04
202		.121	2110	.323	.444	236	2.68	7552	94.6	2.30
205		.121	1470	.570	.691	345	4.73	7095	90.7	2.11
207		.115	1345	.575	.690	360	4.99	7413	95.6	3.98
208		.076	1270	.409	.485	253	5.40	7412	96.9	3.43
210		.073	1105	.515	.588	282	7.02	6815	94.2	----
211		.064	910	.626	.690	303	9.81	6240	95.3	----
212		.056	935	.541	.597	256	9.64	6093	92.4	3.21
213		.049	790	.633	.682	266	12.84	5542	92.5	3.00

(c) Radial-jet injector

[Oxygen flow area, 0.0136 sq in.]

Hydrogen injection plate 2 (nine center holes); area, 0.1868 sq in.										
272	3	0.122	840	0.485	0.607	312	4.00	7402	93.0	----
275		.121	732	.622	.743	358	5.14	6938	89.9	----
274		.082	663	.494	.576	266	6.03	6650	88.8	----
263	12	.127	710	.632	.759	380	4.98	7209	92.9	3.84
262		.126	770	.545	.671	353	4.33	7576	95.8	4.25
268		.123	720	.629	.752	367	5.10	7027	90.9	4.50
267		.123	820	.531	.654	325	4.32	7155	90.5	3.61
215		.122	788	.522	.644	334	4.29	7369	93.2	3.35
261		.098	788	.423	.521	269	4.33	7435	94.1	3.23
269		.081	609	.521	.602	287	6.41	6864	92.9	3.85
264		.081	620	.524	.605	283	6.47	6736	91.3	3.65
270		.080	530	.662	.742	328	8.24	6365	92.1	4.24
Hydrogen injection plate 4 (45 holes); area, 0.6286 sq in.										
258	16	0.125	210	0.631	0.756	377	5.03	7181	92.7	4.08
168		.121	295	.438	.559	265	3.62	6775	84.8	3.53
169		.121	240	.531	.652	323	4.39	7079	89.7	3.88
171		.071	160	.525	.596	277	7.44	6642	93.3	3.42
172		.069	145	.608	.677	302	8.80	6375	94.3	3.09
170		.063	175	.405	.468	231	6.45	7054	95.6	2.97

TABLE I. - Concluded. SUMMARY OF EXPERIMENTAL INJECTOR PERFORMANCE

(d) Impinging-jet, series I injector

[Two impinging liquid-oxygen jets; oxygen flow area, 0.0124 sq in.]

Run	Chamber length, in.	Fuel weight flow, lb/sec	Fuel-injection velocity, ft/sec	Oxidant weight flow, lb/sec	Total weight flow, lb/sec	Chamber pressure, lb/sq in. abs	Oxidant-fuel weight ratio	Characteristic exhaust velocity, C*, ft/sec	Percent of theoretical C*	Heat-transfer rate, Btu/(sec)(sq in.)
Hydrogen injection plate 1 (one center hole); area, 0.0356 sq in.										
82	14	0.1063	Sonic	0.422	0.528	255	3.97	6830	85.8	
77		.0982	3230	.518	.616	306	5.27	7025	91.4	
85		.0977	2935	.604	.702	345	6.18	6950	93.3	
78		.0988	2915	.610	.707	344	6.30	6881	92.0	
86		.0705	3190	.353	.424	224	5.01	7470	96.4	
88		.0666	2435	.567	.634	291	8.51	6490	94.6	
Hydrogen injection plate 2 (nine center holes); area, 0.1868 sq in.										
291	3	0.126	805	0.607	0.733	337	4.82	6610	84.7	
290		.126	1240	.285	.411	217	2.27	7601	96.1	
286		.125	1150	.367	.492	233	2.93	6787	84.8	
285		.125	1150	.363	.488	233	2.90	6857	85.7	
287		.116	870	.519	.635	289	4.46	6525	82.8	
288		.083	860	.391	.474	207	4.72	6284	80.3	
292		.082	600	.651	.733	295	7.91	5780	82.6	
289		.077	655	.519	.596	255	6.78	6096	83.5	
68	8	.125	860	.521	.646	315	4.17	7344	92.6	
69		.125	785	.616	.741	344	4.93	7000	90.1	
70		.125	730	.696	.821	371	5.57	6810	89.5	
40	14	.126	898	.446	.572	303	3.54	7628	95.4	
39		.125	1080	.348	.473	253	2.78	7699	96.4	
42		.125	720	.628	.753	373	5.02	7138	98.4	
48		.124	1120	.323	.447	237	2.61	7625	95.7	
41		.123	785	.535	.658	340	4.35	7442	94.2	
49		.123	940	.421	.544	281	3.42	7436	92.9	
55		.087	540	.718	.805	348	8.25	6234	90.1	
53		.086	645	.539	.625	288	6.27	6631	89.2	
54		.086	590	.623	.709	316	7.25	6427	89.6	
58	22	.127	965	.427	.554	283	3.36	7494	93.6	
59		.125	835	.509	.634	324	4.07	7481	94.2	
60		.119	715	.600	.719	358	5.04	7289	94.1	
61		.119	675	.679	.798	380	5.70	6980	92.2	
63		.080	600	.535	.615	289	6.68	6881	94.0	
64		.079	525	.637	.716	325	8.06	6650	95.5	
65		.070	490	.668	.738	306	9.54	6087	92.0	
Hydrogen injection plate 3 (16 peripheral holes); area, 0.1963 sq in.										
91	14	0.122	835	0.543	0.665	300	4.45	6415	81.4	
92		.121	705	.677	.798	352	5.58	6272	82.5	
97		.081	555	.643	.724	298	7.89	5853	83.5	
98		.070	450	.757	.827	315	10.80	5416	85.4	
99		.061	415	.770	.831	303	12.54	5179	85.8	
104	22	.122	690	.570	.692	363	4.68	7460	95.2	
103		.122	795	.490	.612	315	4.03	7319	92.1	
101		.122	920	.387	.509	273	3.18	7626	95.2	
100		.120	1010	.321	.441	242	2.67	7804	97.8	
Hydrogen injection plate 4 (45 holes); area, 0.6286 sq in.										
251	3	0.123	330	0.471	0.594	239	3.82	5795	72.7	----
253		.121	375	.388	.509	207	3.21	5856	73.1	----
252		.101	235	.599	.700	278	5.95	5718	76.1	----
255		.080	198	.629	.709	264	7.83	5363	76.3	----
254		.080	250	.474	.554	205	5.95	5328	20.9	----
151	12	.123	245	.518	.641	318	4.22	7035	88.8	3.47
150		.122	280	.432	.554	278	3.55	7103	88.8	3.08
149		.121	320	.337	.458	239	2.80	7399	92.5	2.53
153		.079	220	.390	.469	224	4.92	6772	87.2	2.49
154		.079	190	.499	.578	287	6.34	6550	88.4	2.62
158	24	.119	240	.508	.627	319	4.26	7271	91.9	4.48
157		.119	275	.423	.542	278	3.55	7329	91.7	3.04
159		.119	210	.590	.709	360	4.97	7256	93.5	4.56
165		.078	265	.629	.707	324	8.04	6549	94.0	3.34
166		.078	195	.483	.561	271	6.18	6903	92.6	3.37

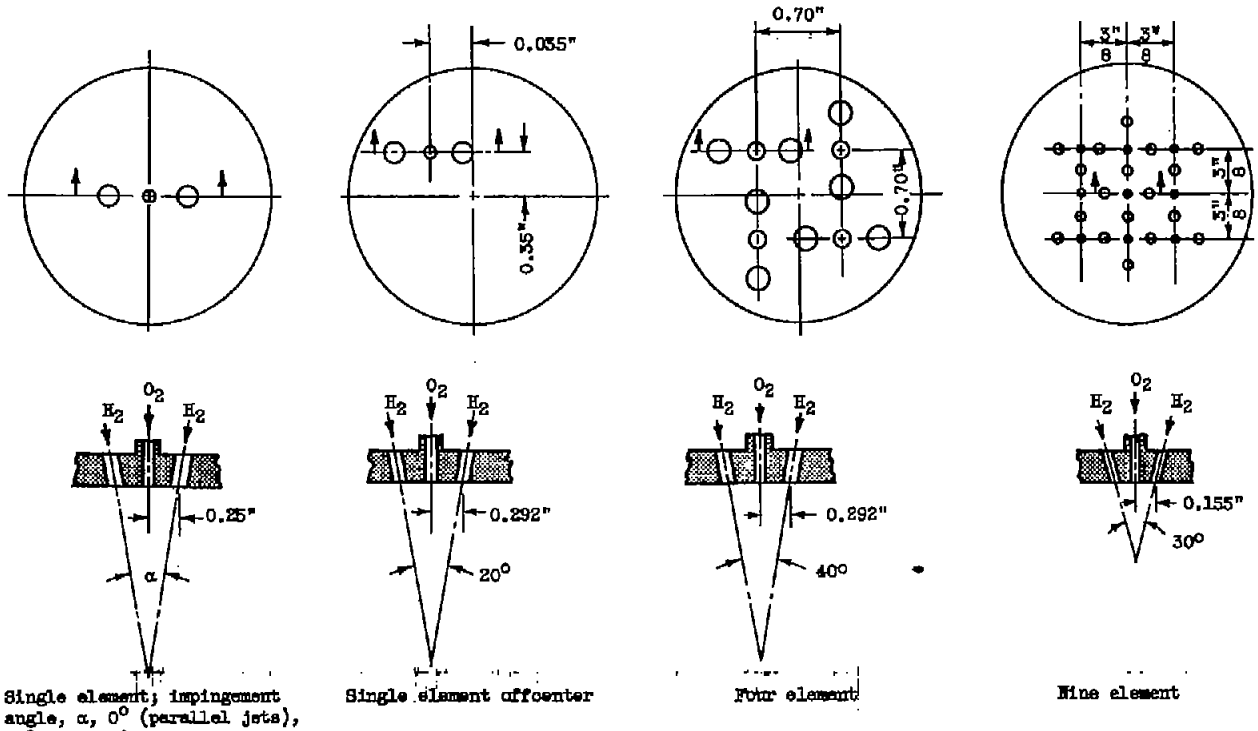

Single element; impingement angle, α, 0° (parallel jets), 20°, and 40°

Single element offcenter

Four element

Nine element

Total flow area, sq in. Oxygen Hydrogen	0.0075 .0433	0.0075 .0433	0.0302 .1731	0.0113 .0951
Orifice diam., in. Oxygen Hydrogen	0.0975 .186	0.0975 .186	0.0975 .166	0.040 .082
Hydrogen-injection velocity, ft/sec (0.12 lb/sec)	5292	3293	925	1645

(a) Triplet injector.

Figure 1. - Injector designs.

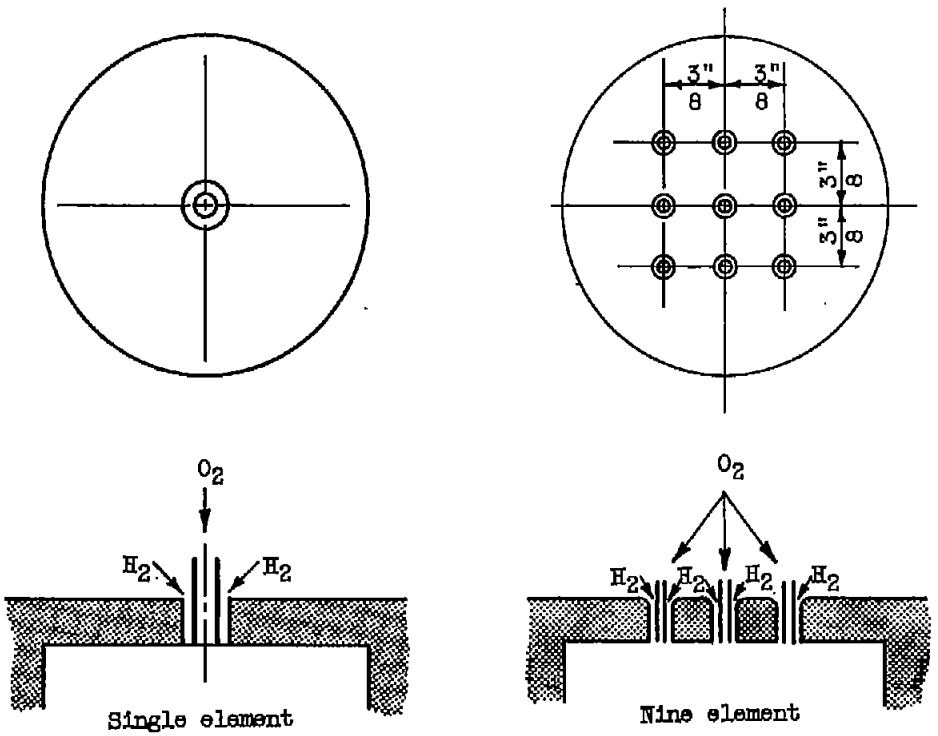

Total flow area, sq in. Oxygen Hydrogen	0.0108 .0490	0.0113 .0939
Oxygen orifice diam., in. Hydrogen annular width, in.	0.117 .0625	0.040 .044
Hydrogen-injection velocity, ft/sec (0.12 lb/sec)	2985	1675

(b) Concentric-tube injector.

Figure 1. - Continued. Injector designs.

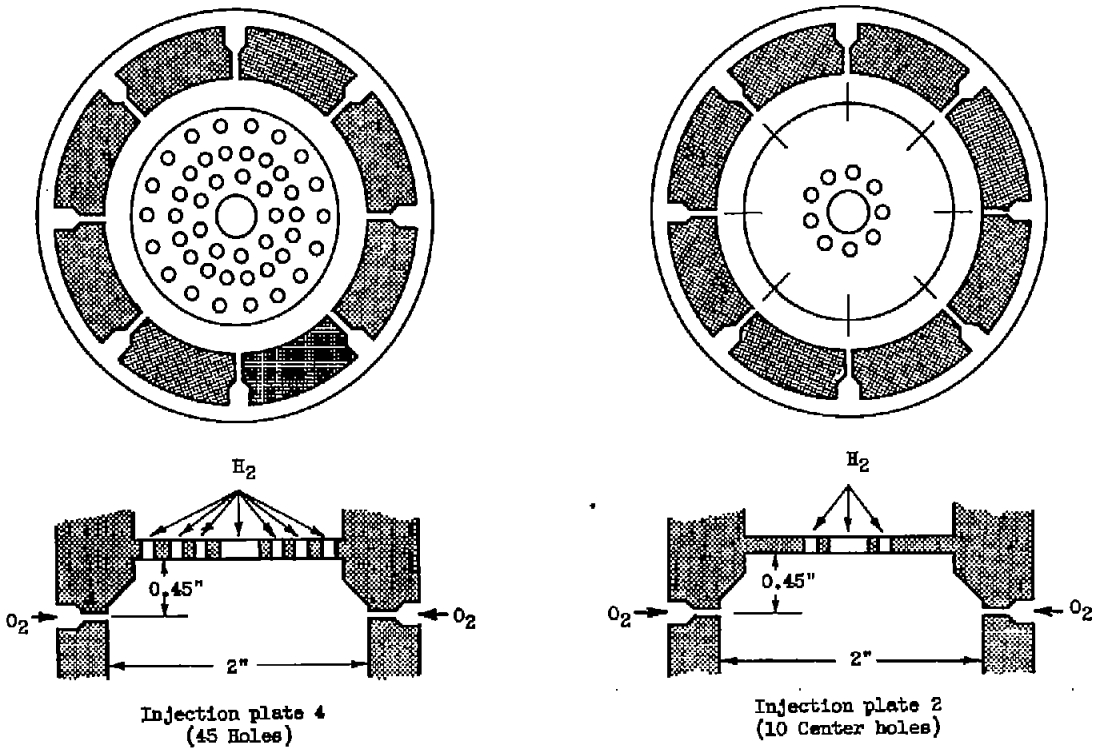

Injection plate 4 (45 Holes)

Injection plate 2 (10 Center holes)

Total flow area, sq in. Oxygen Hydrogen	0.0136 .6286	0.0136 .1868
Orifice diam., in. Oxygen	0.0466	0.0466
Hydrogen	0.125 (44 Holes) .3125 (One hole)	0.125 (Nine holes) .3125 (One hole)
Hydrogen-injection velocity, ft/sec (0.12 lb/sec)	255	860

(c) Radial-jet injector.

Figure 1. - Continued. Injector designs.

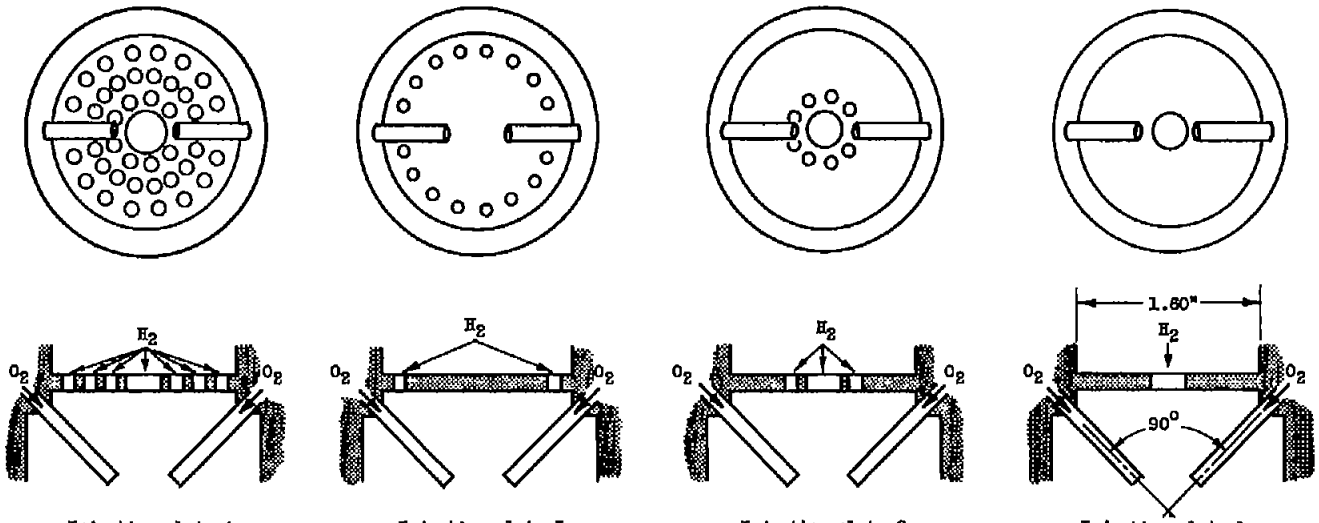

	Injection plate 4 (45 Holes)	Injection plate 3 (18 Peripheral holes)	Injection plate 2 (10 Center holes)	Injection plate 1 (One center hole)
Total flow area, sq in.				
Oxygen	0.0124	0.0124	0.0124	0.0124
Hydrogen	.6286	.1985	.1868	.0358
Orifice diam., in.				
Oxygen	0.089	0.089	0.089	0.089
Hydrogen	0.125 (44 Holes) .3125 (One hole)	0.125	0.125 (Nine holes) .3125 (One hole)	0.212
Hydrogen-injection velocity, ft/sec (0.12 lb/sec)	255	820	880	3820

(d) Impinging oxygen-jet injector.

Figure 1. - Concluded. Injector designs.

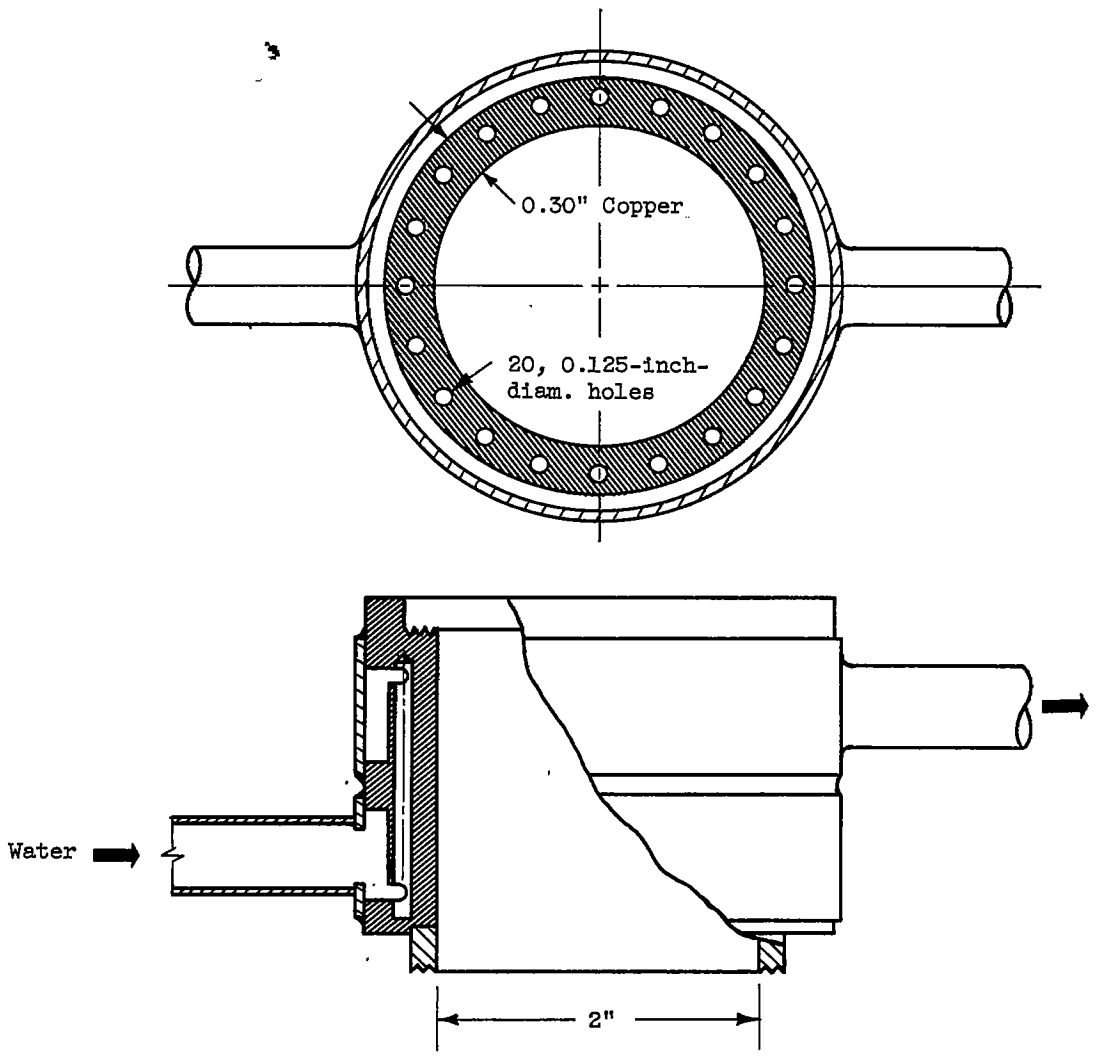

Figure 2. - Water-cooled chamber segment used for heat-rejection measurements showing section view of coolant passages.

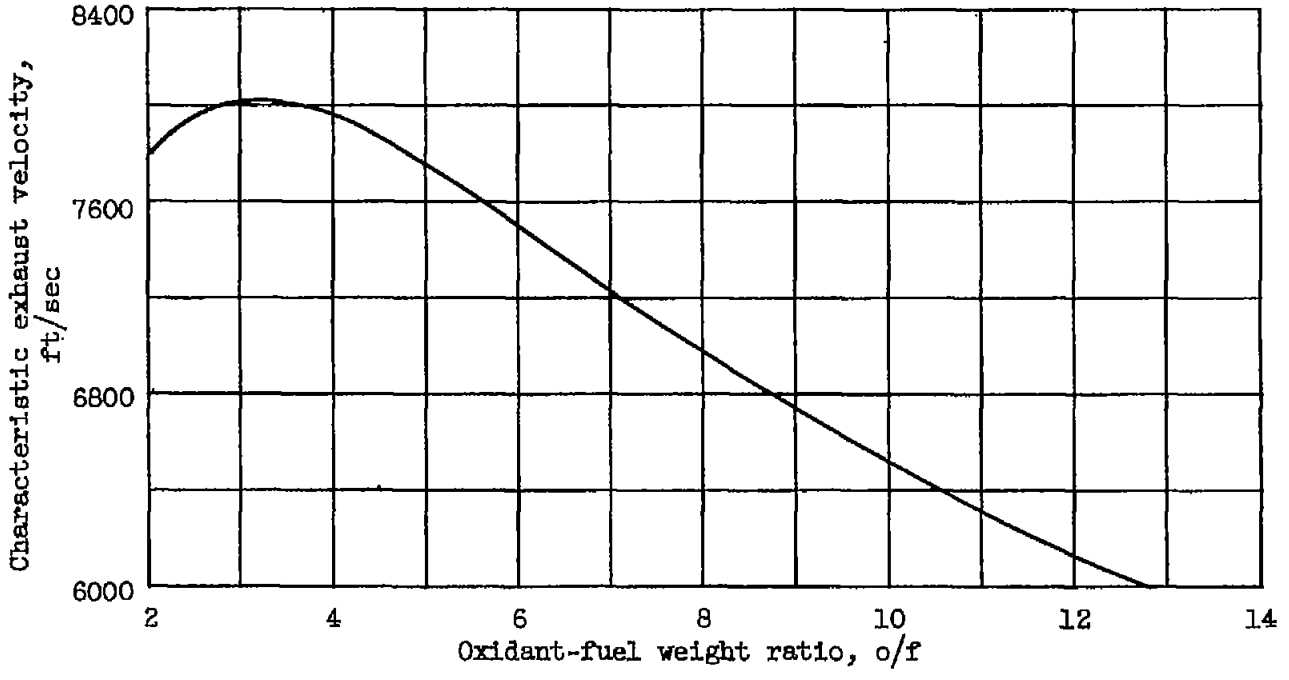

Figure 3. - Theoretical variation of characteristic exhaust velocity with mixture ratio for hydrogen and oxygen.

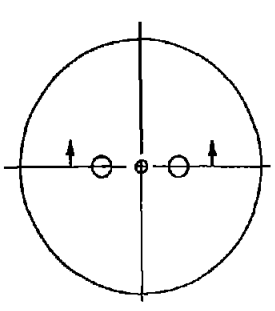

Single element; impingement angle, α, 0° (parallel jets), 20°, and 40°

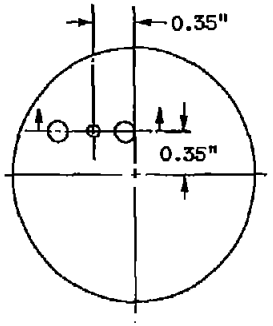

Single element offcenter; impingement angle, α, 20°

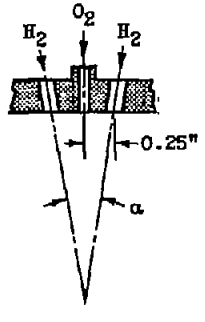

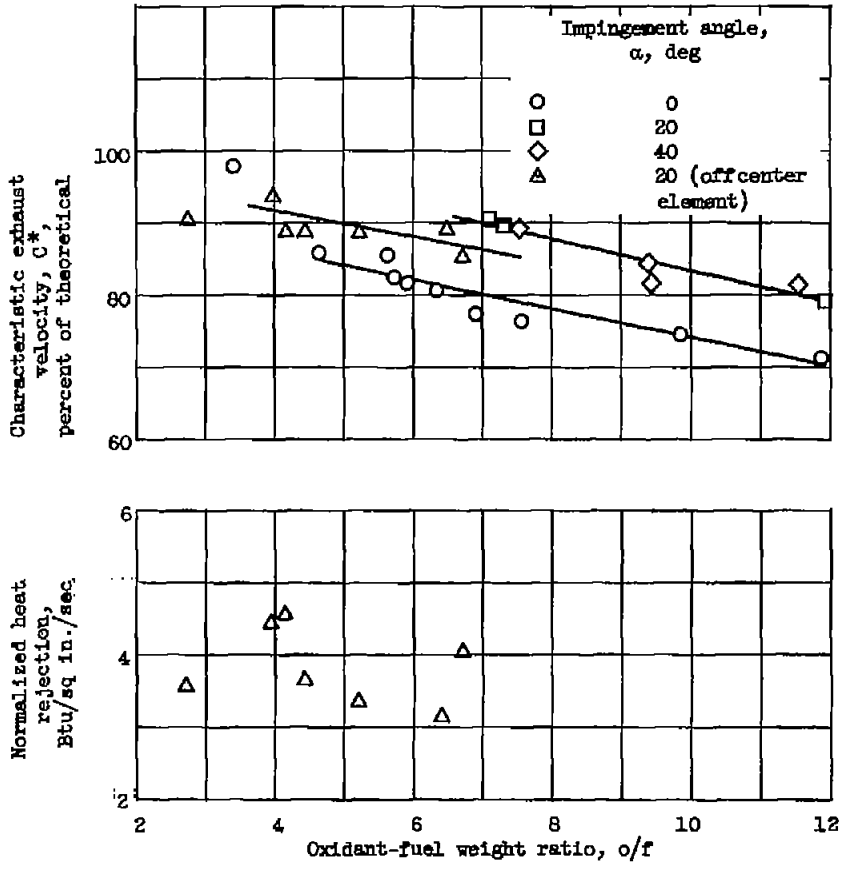

(a) Single-element configuration; chamber length, 12 inches.

Figure 4. - Performance of triplet injectors.

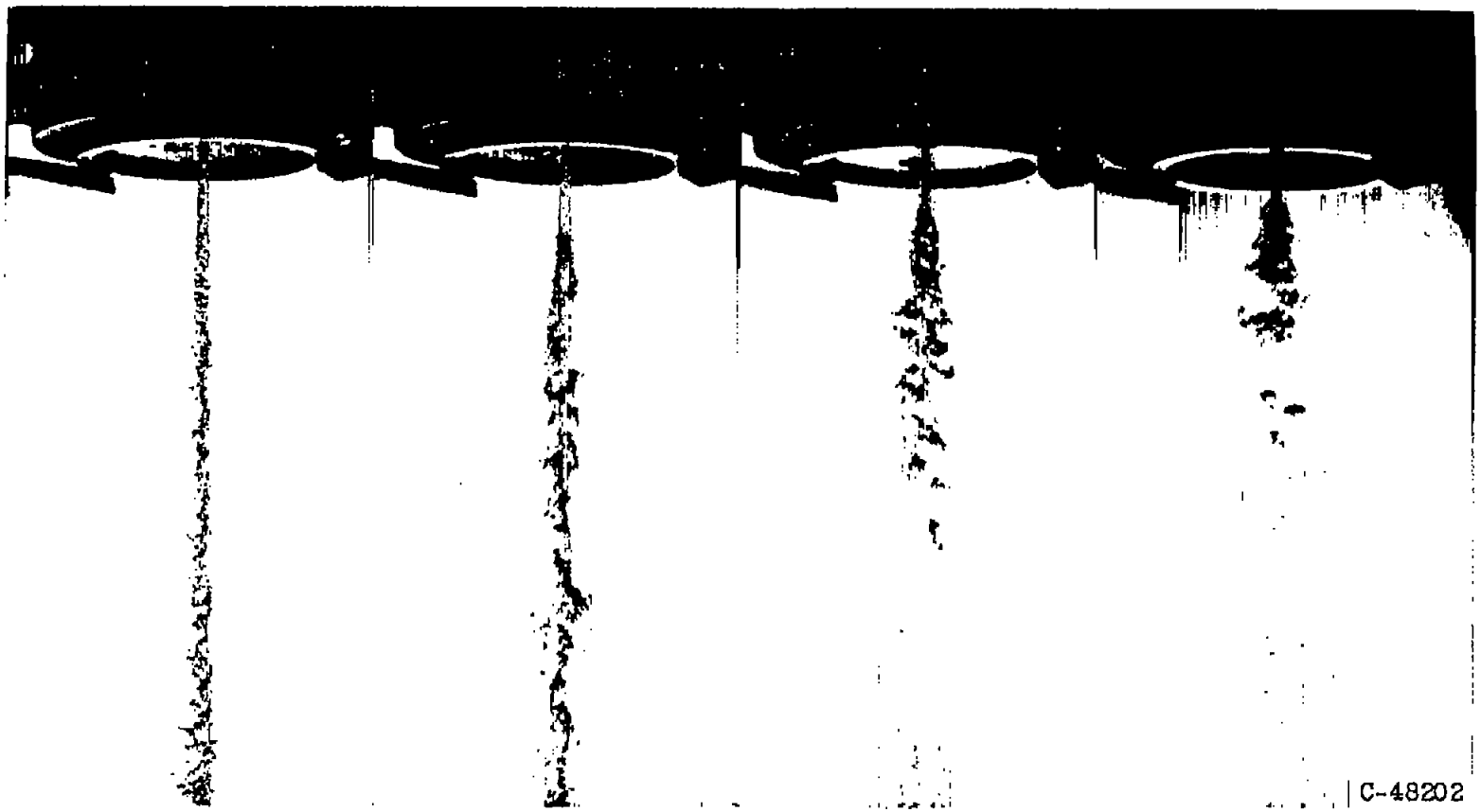

No airflow | Impingement angle, 0° | Impingement angle, 20° | Impingement angle, 40°

(b) Single-element configuration. Flow rates: water, 0.211 pound per second; air, 0.036 pound per second.

Figure 4. - Continued. Performance of triplet injectors.

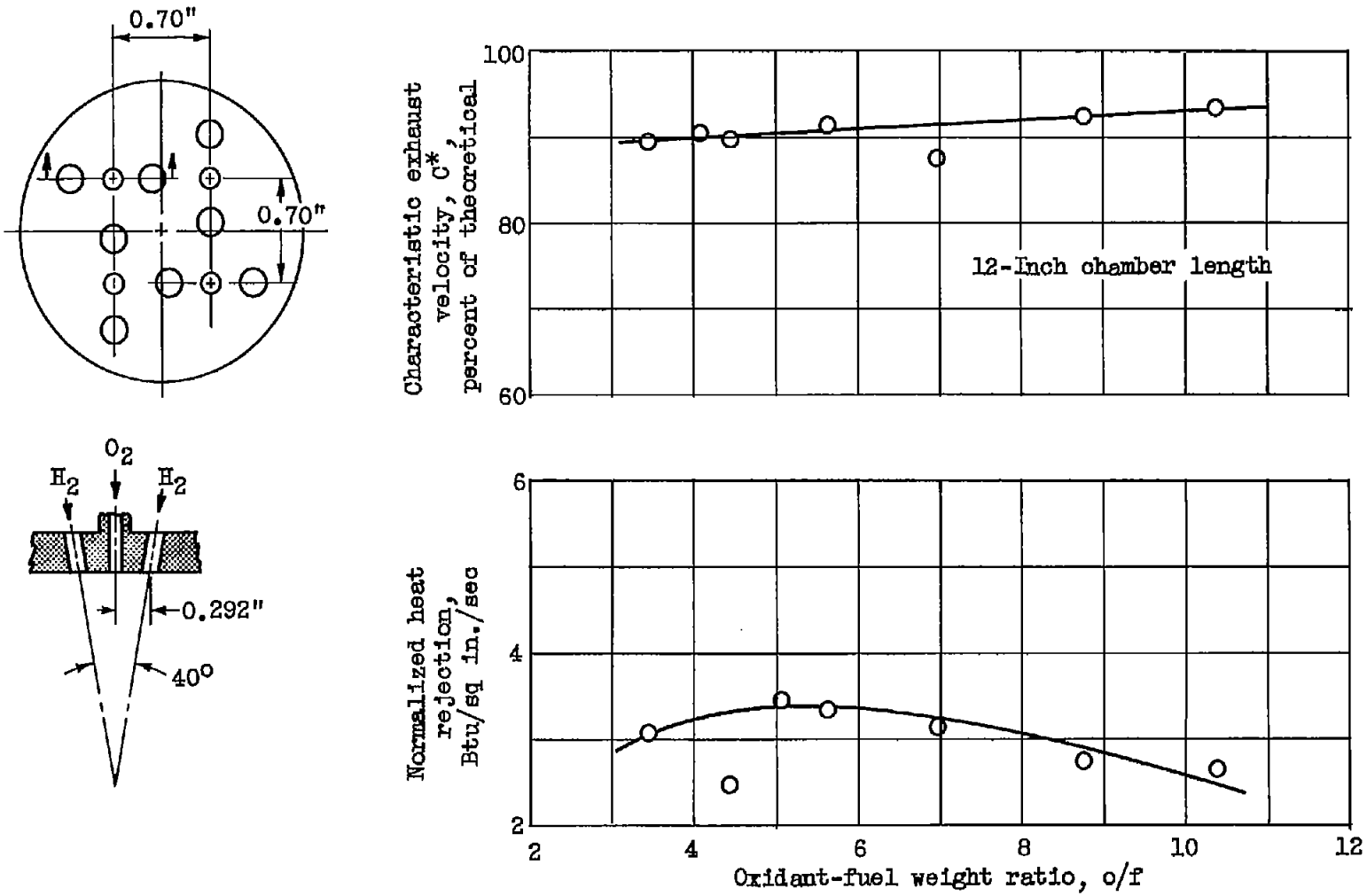

(c) Four-element configuration.

Figure 4. - Continued. Performance of triplet injectors.

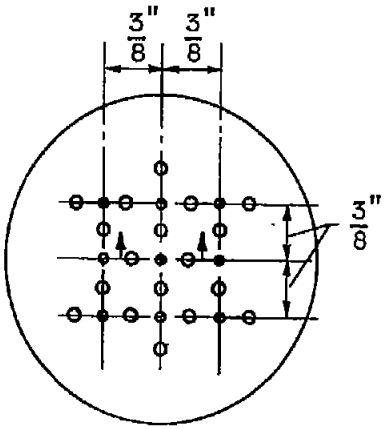

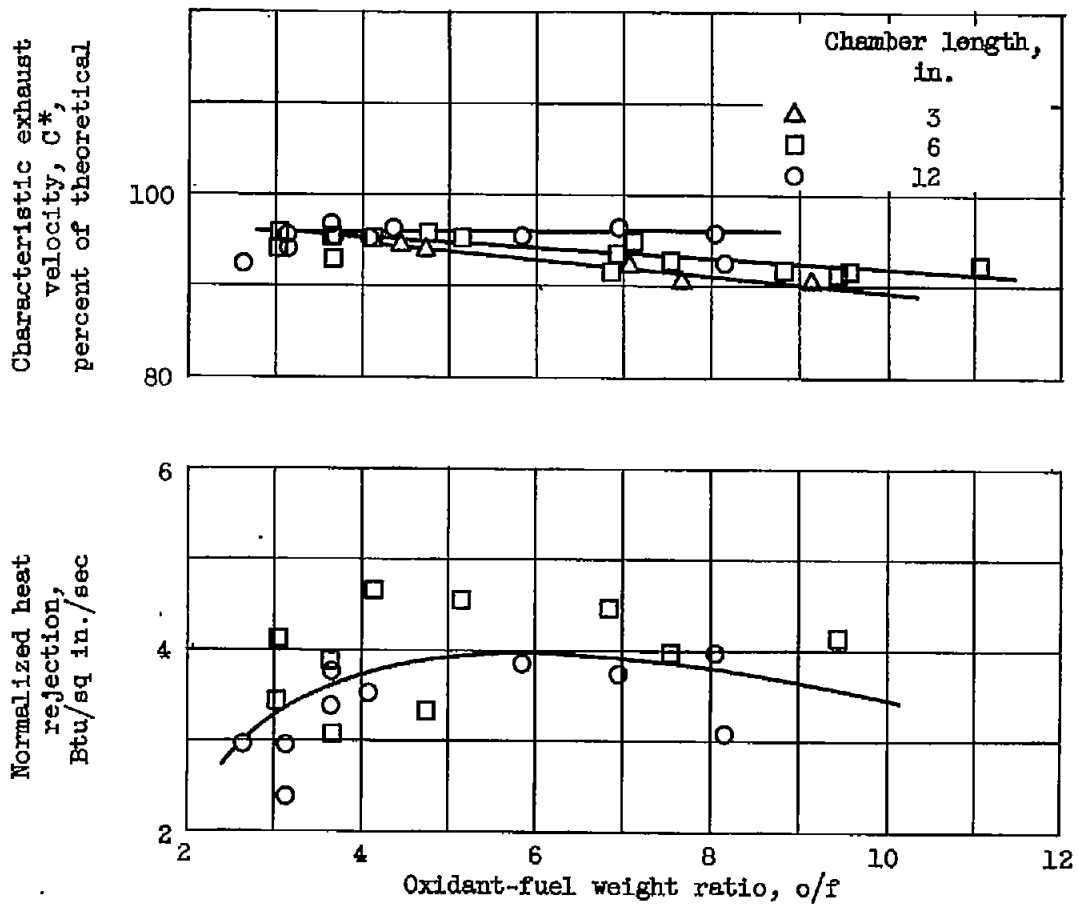

(d) Nine-element configuration.

Figure 4. - Continued. Performance of triplet injectors.

(e) Nine-element configuration. Flow rates: water, 0.370 pound per second; air, 0.058 pound per second.

Figure 4. - Concluded. Performance of triplet injectors.

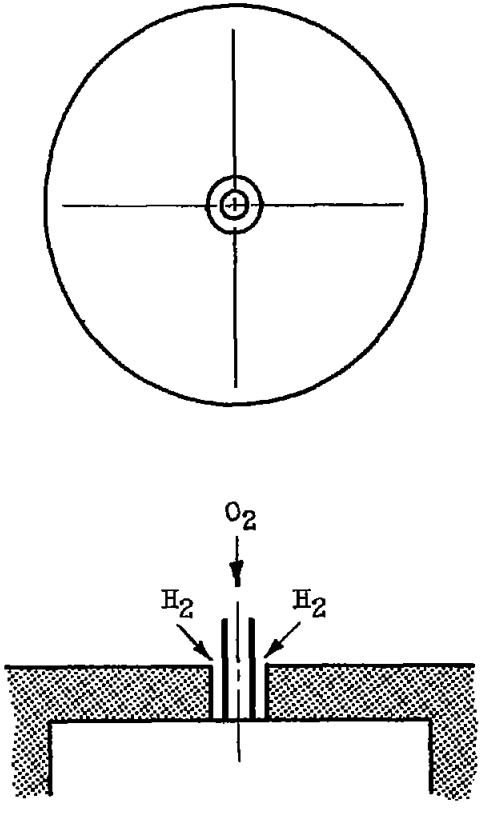

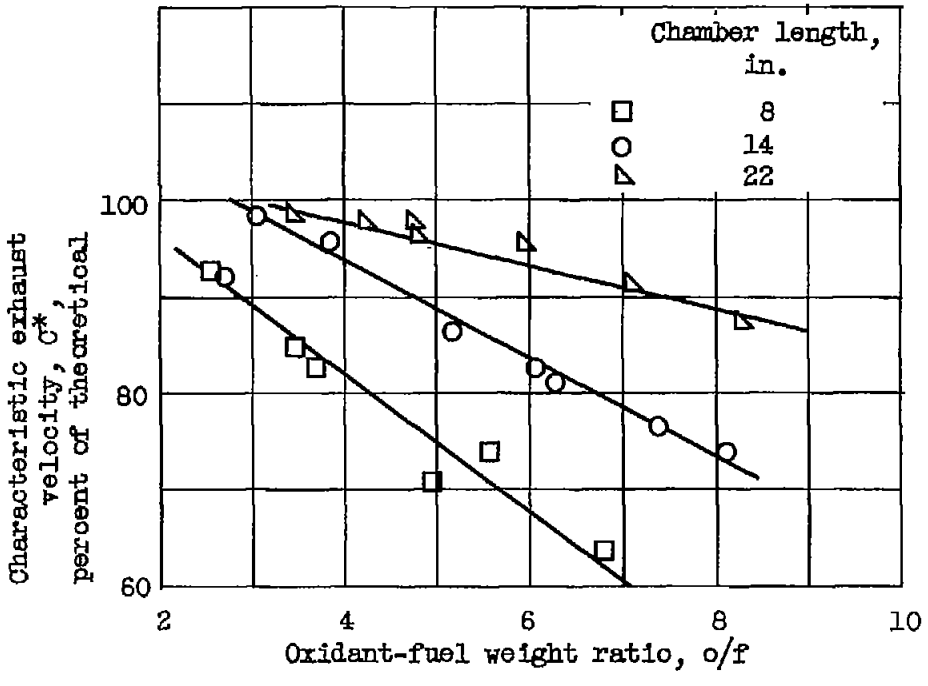

(a) Single-element configuration.

Figure 5. - Performance of concentric-tube injector.

(b) Single-element configuration. Flow rates: water, 0.330 pound per second; air, 0.040 pound per second.

Figure 5. - Continued. Performance of concentric-tube injector.

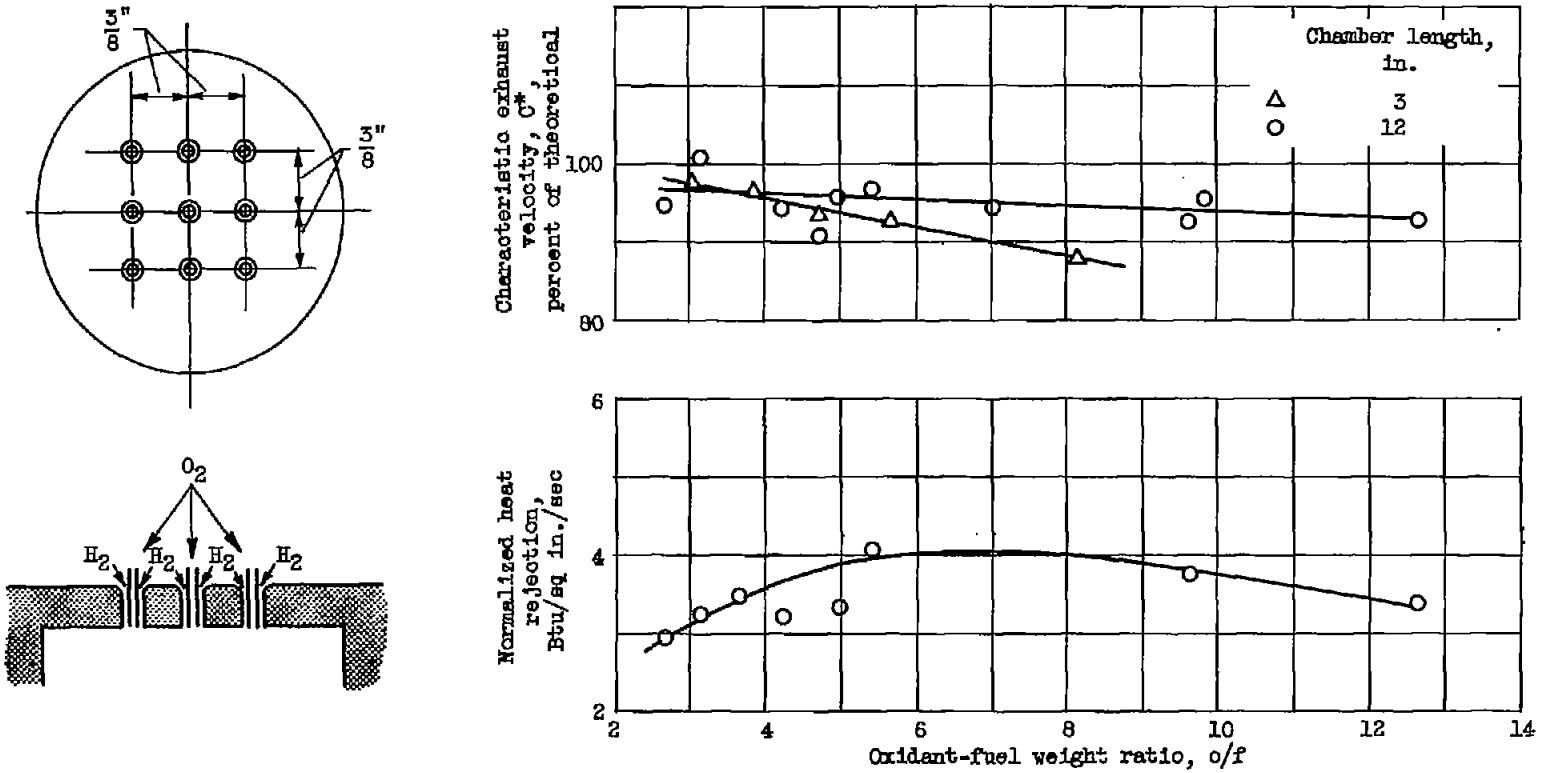

(c) Nine-element configuration.

Figure 5. - Continued. Performance of concentric-tube injector.

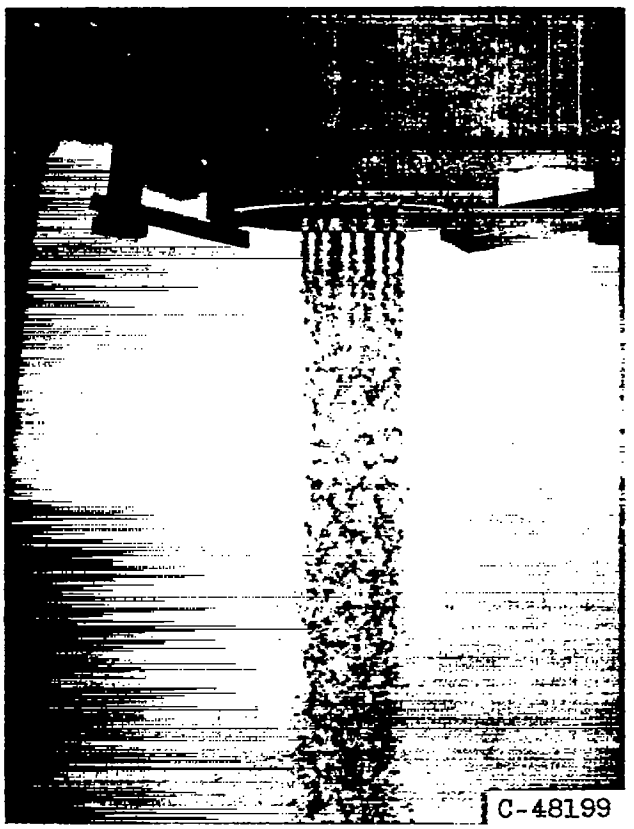

(d) Nine-element configuration. Flow rates: water, 0.370 pound per second; air, 0.032 pound per second.

Figure 5. - Concluded. Performance of concentric-tube injector.

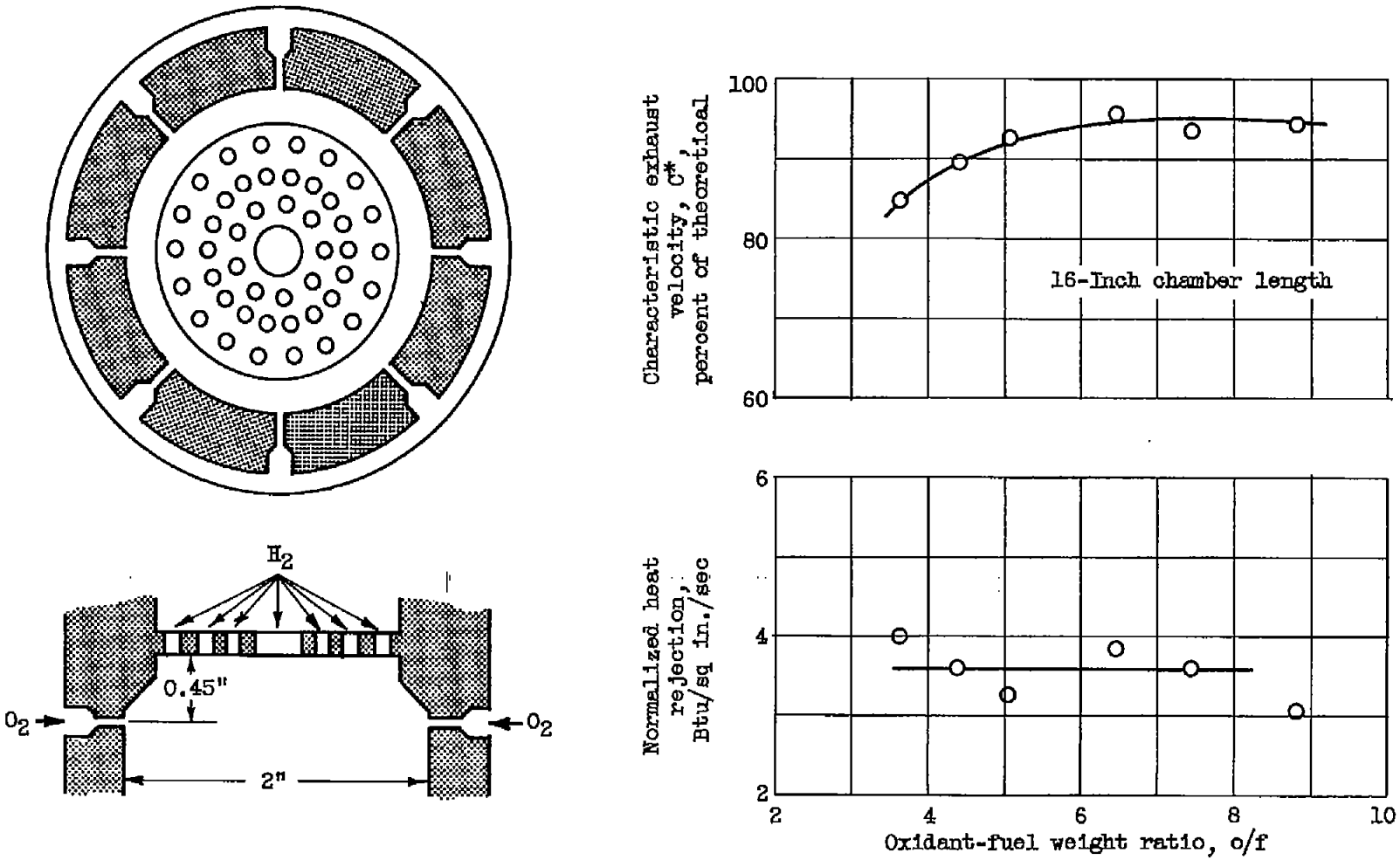

(a) 45-Distributed-hole plate.

Figure 6. - Performance of radial-jet injectors.

(b) 45-Distributed-hole plate. Flow rates: water, 0.320 pound per second; air, 0.107 pound per second.

Figure 6. - Continued. Performance of radial-jet injectors.

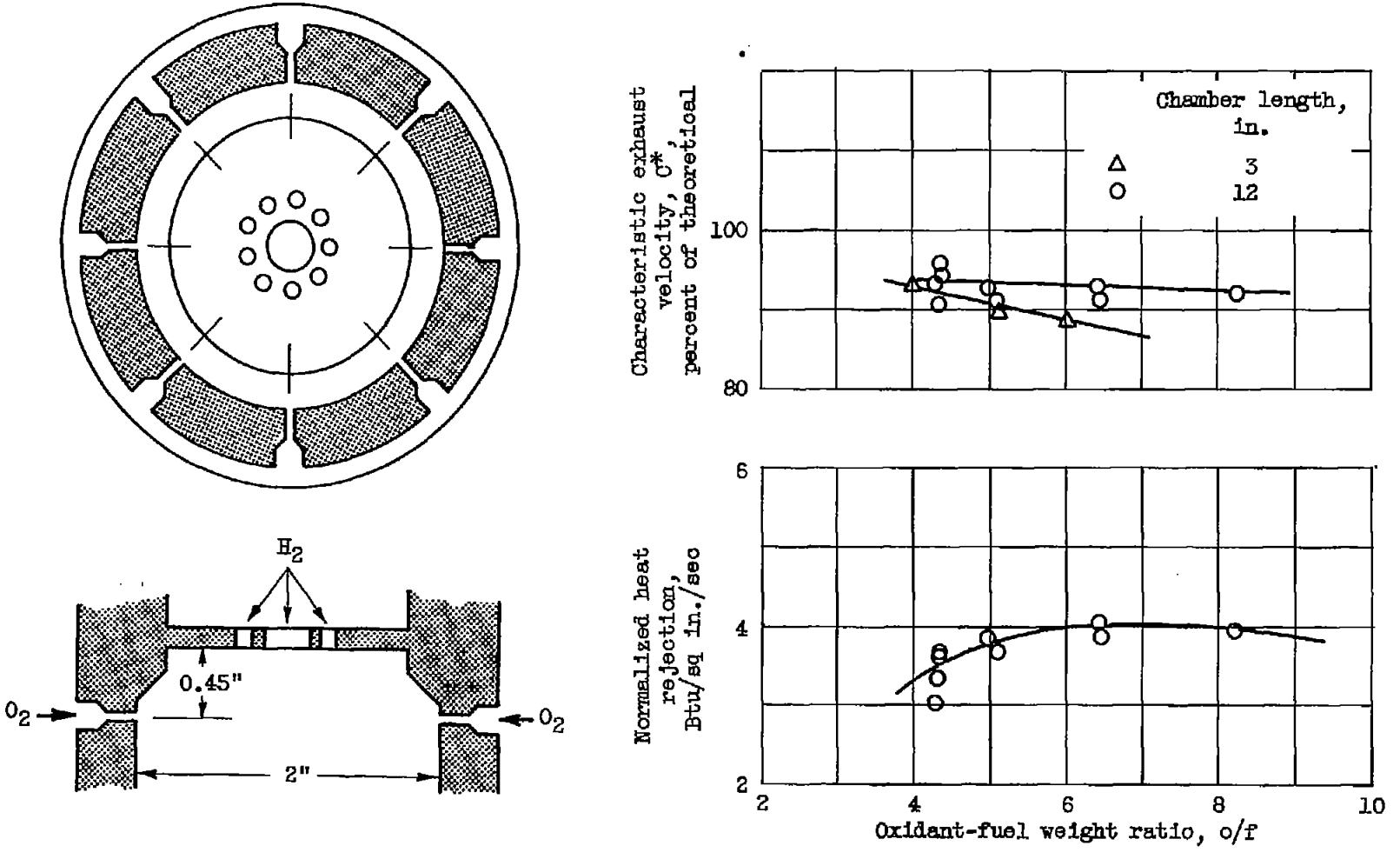

(c) Nine-center-hole plate.

Figure 6. - Continued. Performance of radial-jet injectors.

(d) Nine-center-hole plate. Flow rates: water, 0.320 pound per second; air, 0.105 pound per second.

Figure 6. - Concluded. Performance of radial-jet injectors.

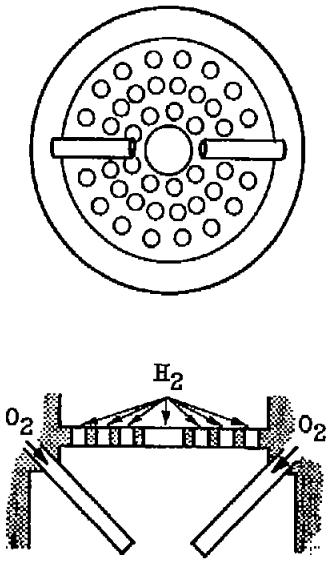

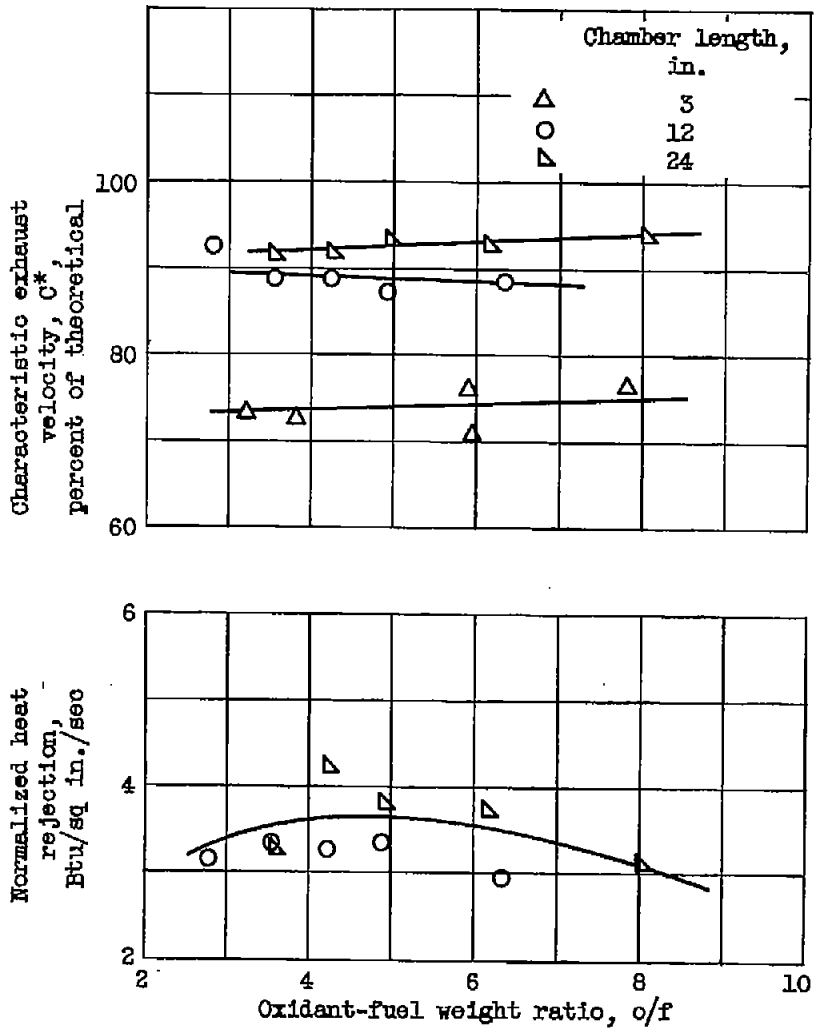

(a) 45-Distributed-hole plate.

Figure 7. - Performance of impinging oxygen-jet injectors.

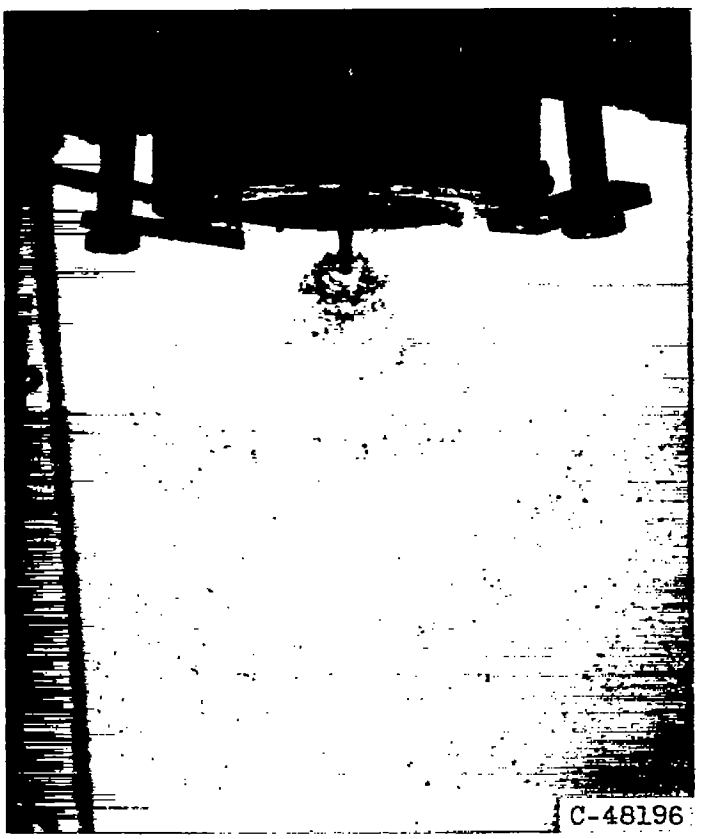

(b) 45-Distributed-hole plate. Flow rates: water, 0.305 pound per second; air, 0.110 pound per second.

Figure 7. - Continued. Performance of impinging oxygen-jet injectors.

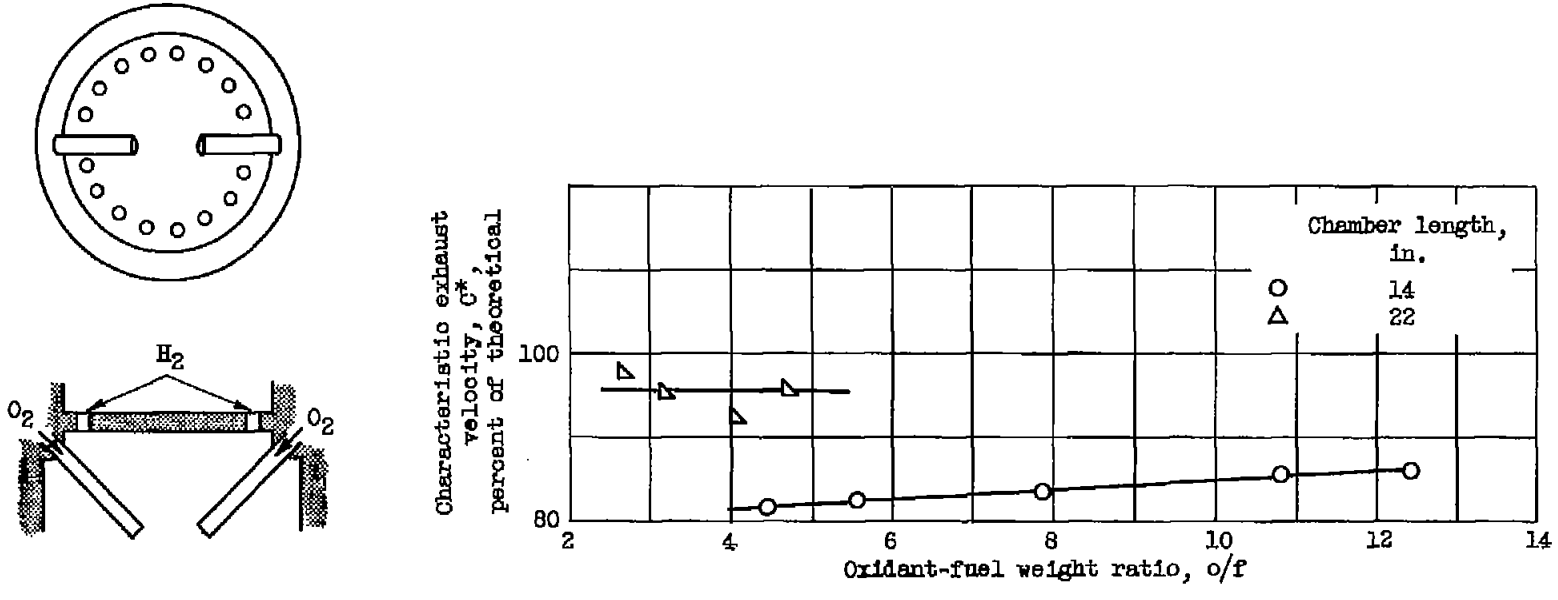

(c) 16-Peripheral-hole plate.

Figure 7. - Continued. Performance of impinging oxygen-jet injectors.

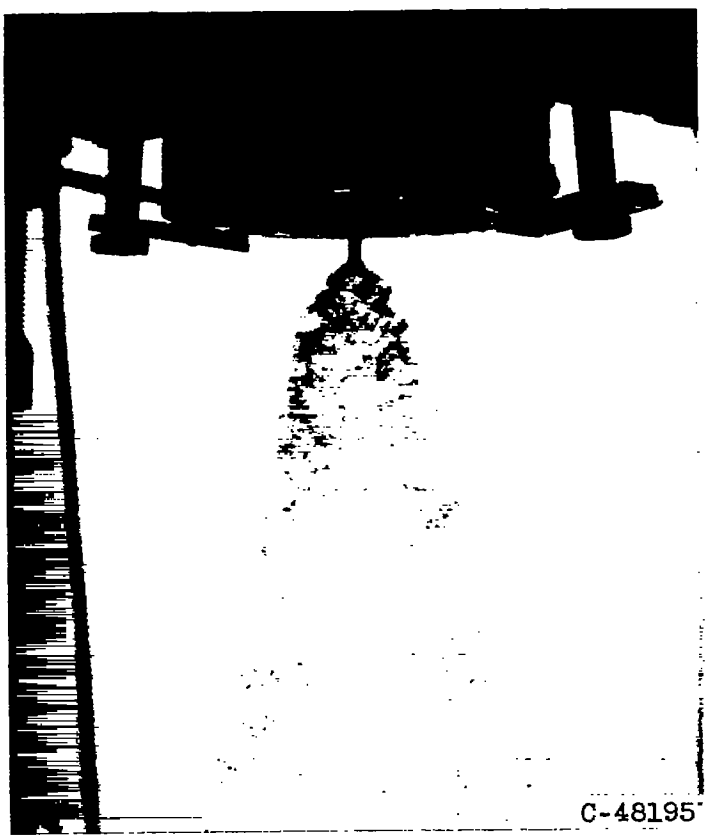

(d) 16-Peripheral-hole plate. Flow rates: water, 0.305 pound per second; air, 0.107 pound per second.

Figure 7. - Continued. Performance of impinging oxygen-jet injectors.

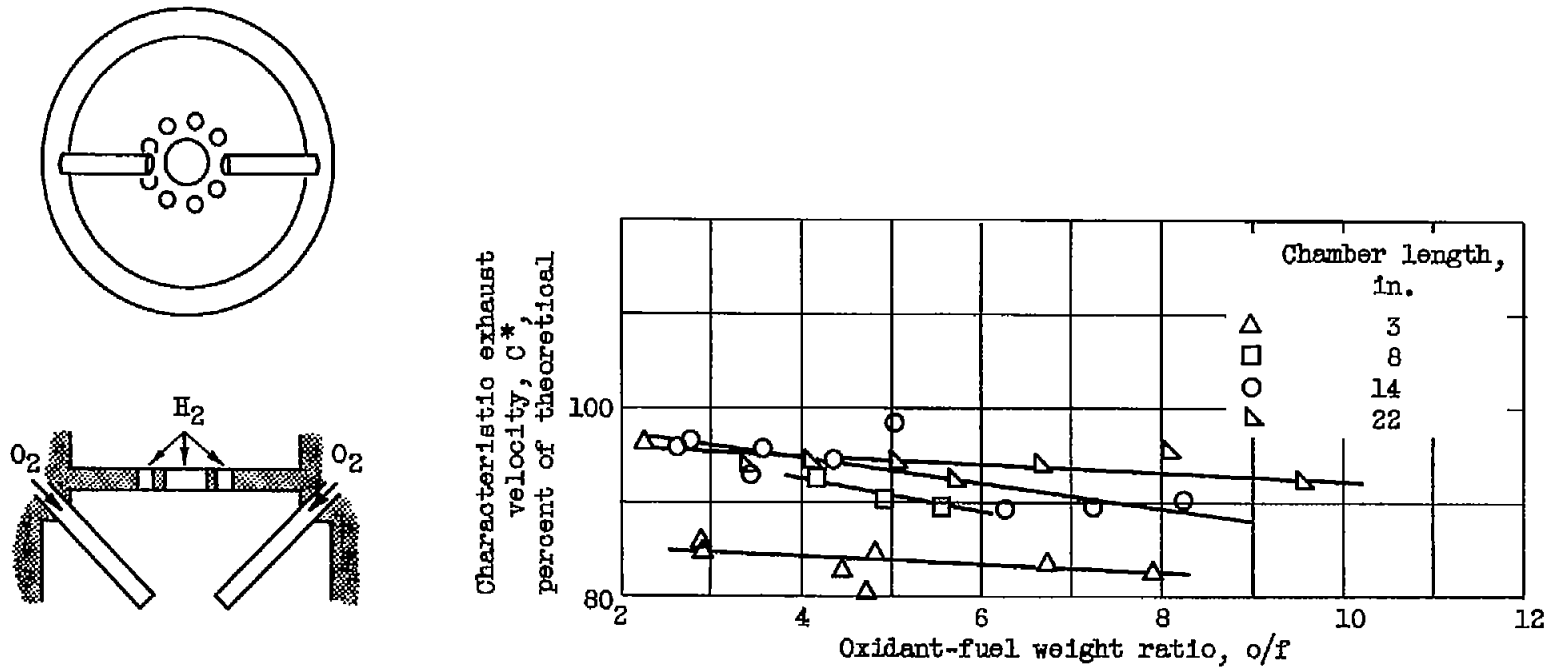

(e) Nine-center-hole plate.

Figure 7. - Continued. Performance of impinging oxygen-jet injectors.

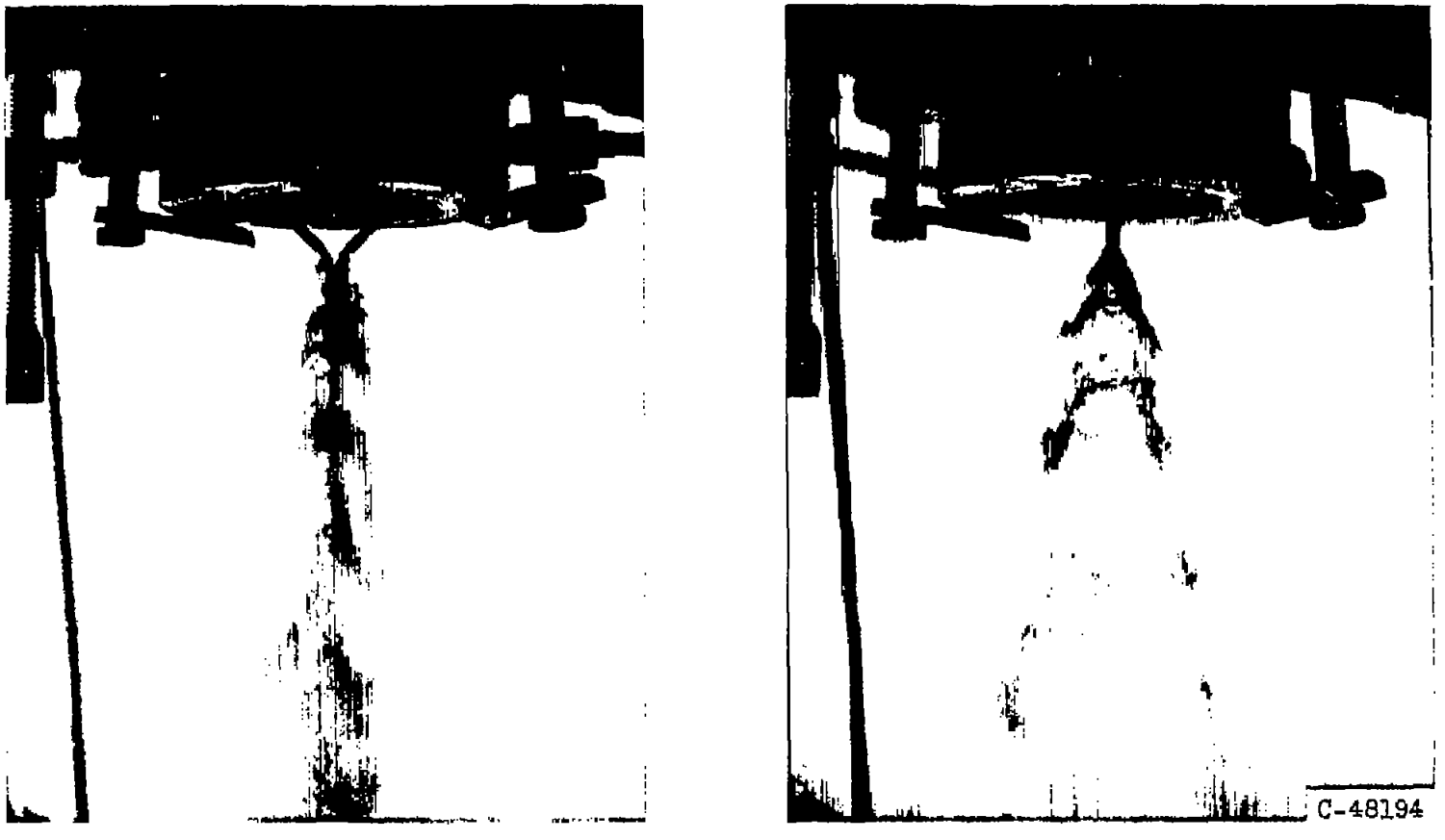

(f) Nine-center-hole plate. Flow rates: water, 0.300 pound per second; air, 0.103 pound per second.

Figure 7. - Continued. Performance of impinging oxygen-jet injectors.

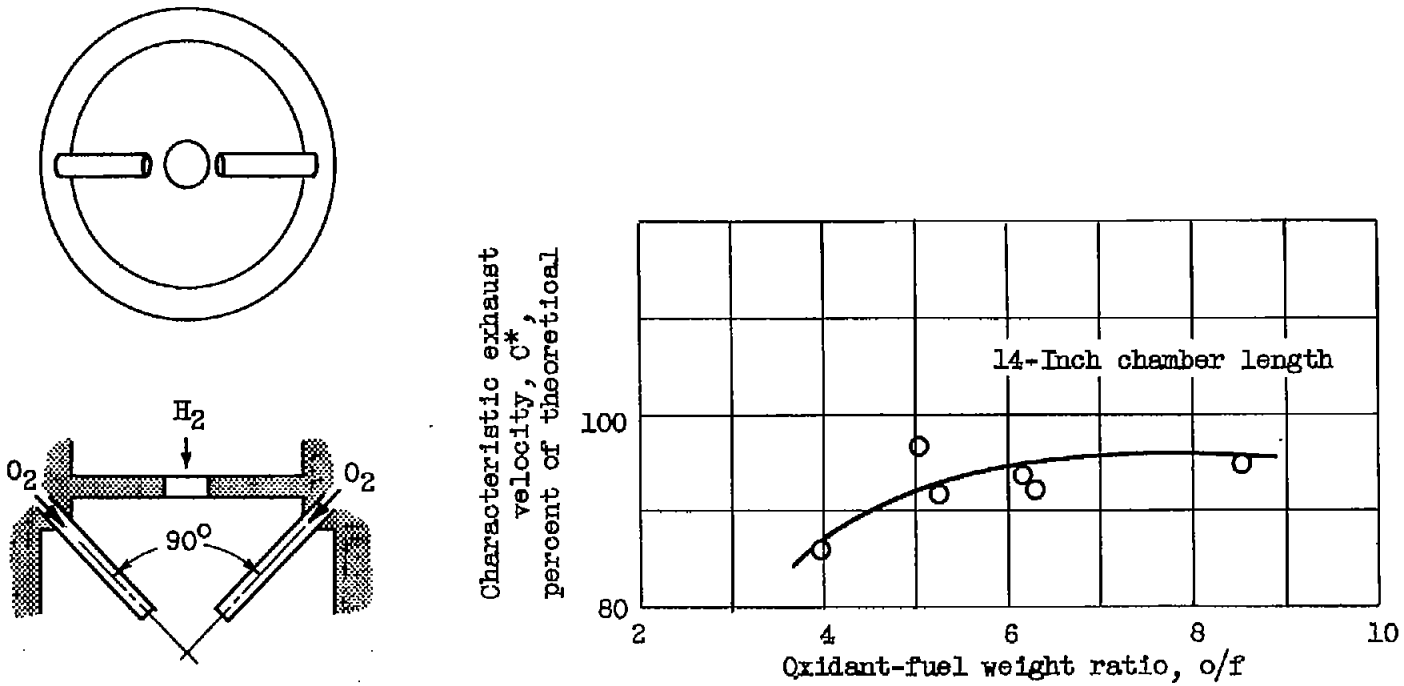

(g) One-center-hole plate.

Figure 7. - Continued. Performance of impinging oxygen-jet injectors.

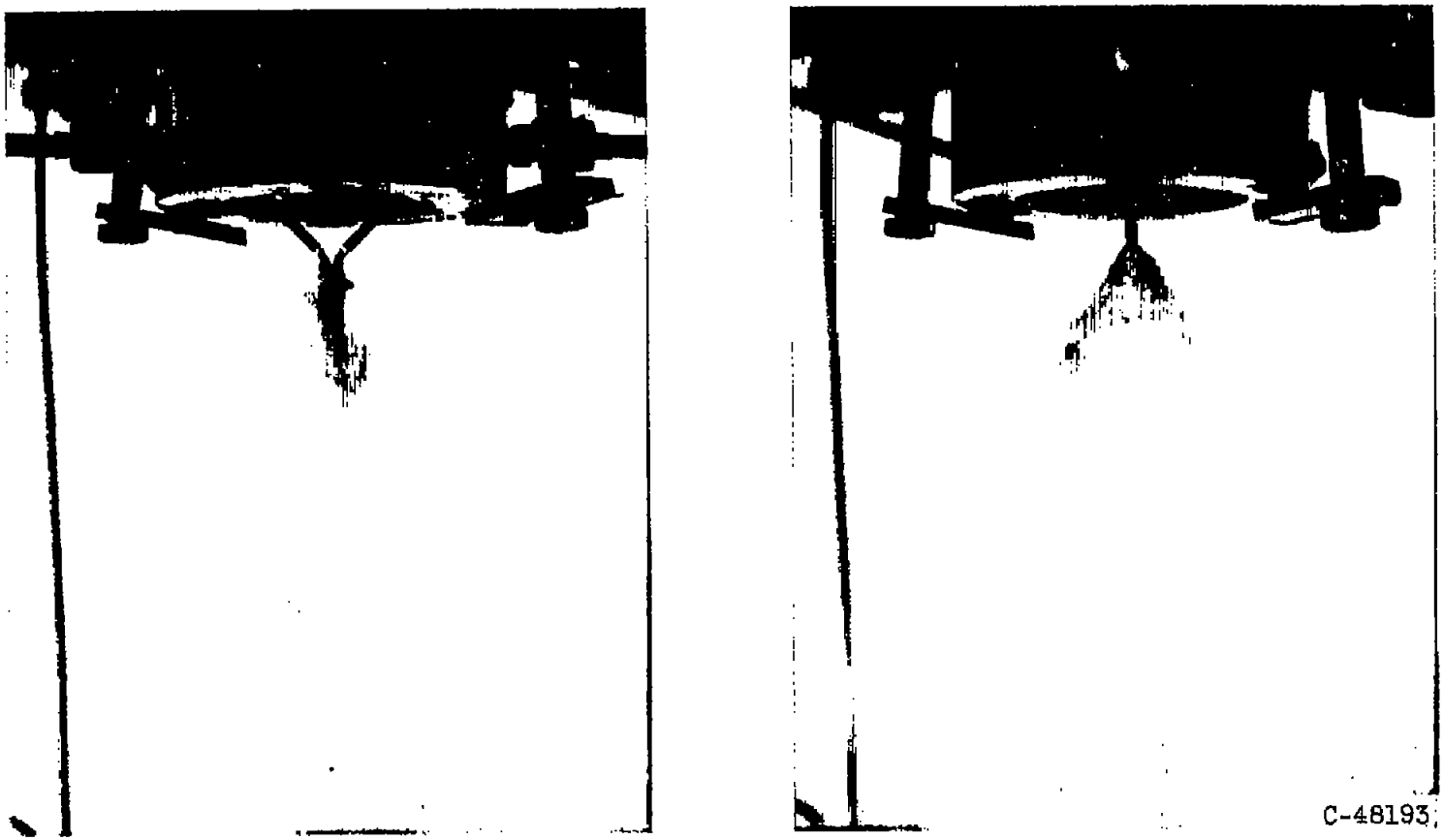

(h) One-center-hole plate. Flow rates: water, 0.305 pound per second; air. 0.020 pound per second.

Figure 7. - Concluded. Performance of impinging oxygen-jet injectors.

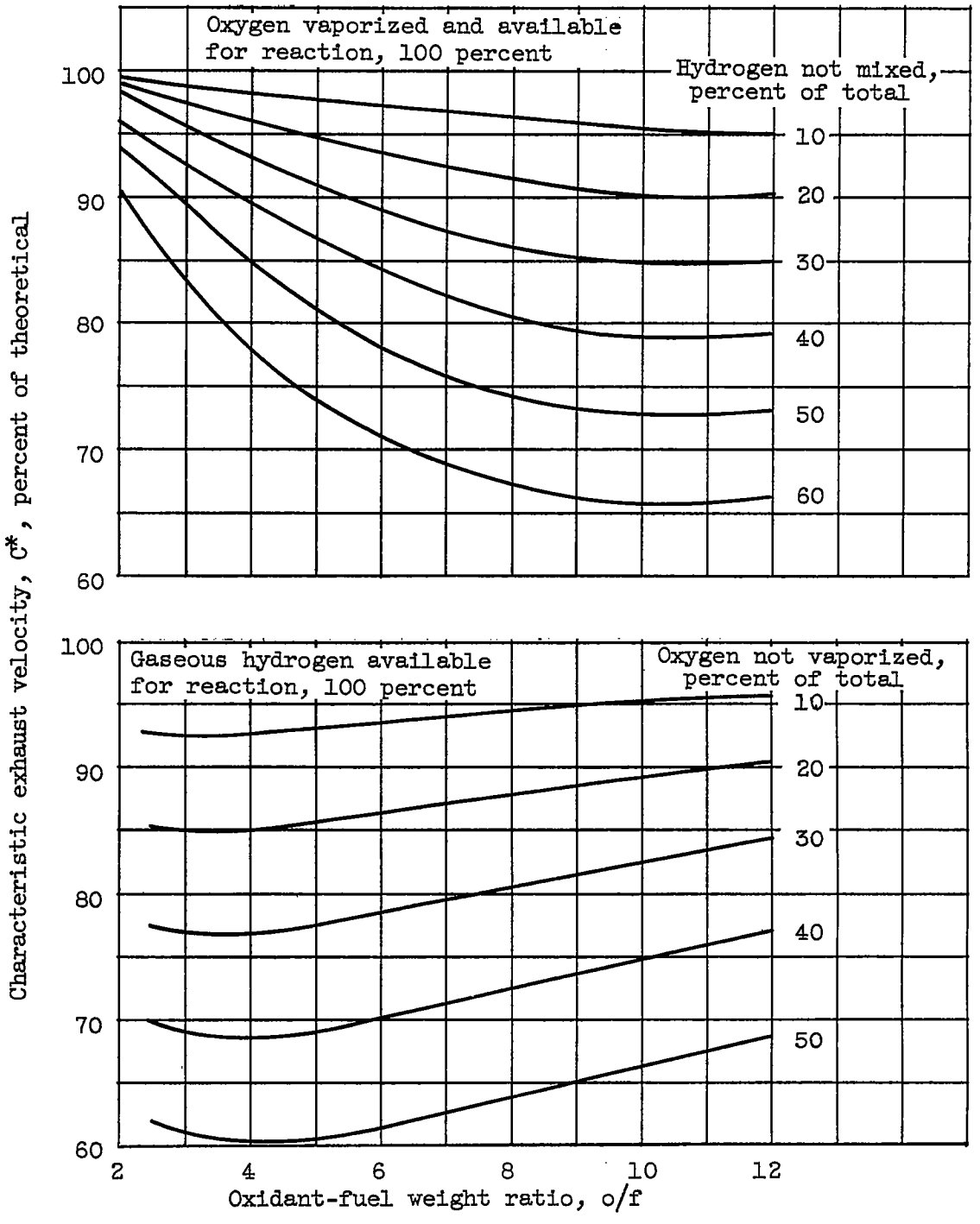

Figure 8. - The effect of incomplete oxygen vaporization and incomplete hydrogen mixing on characteristic exhaust velocity.

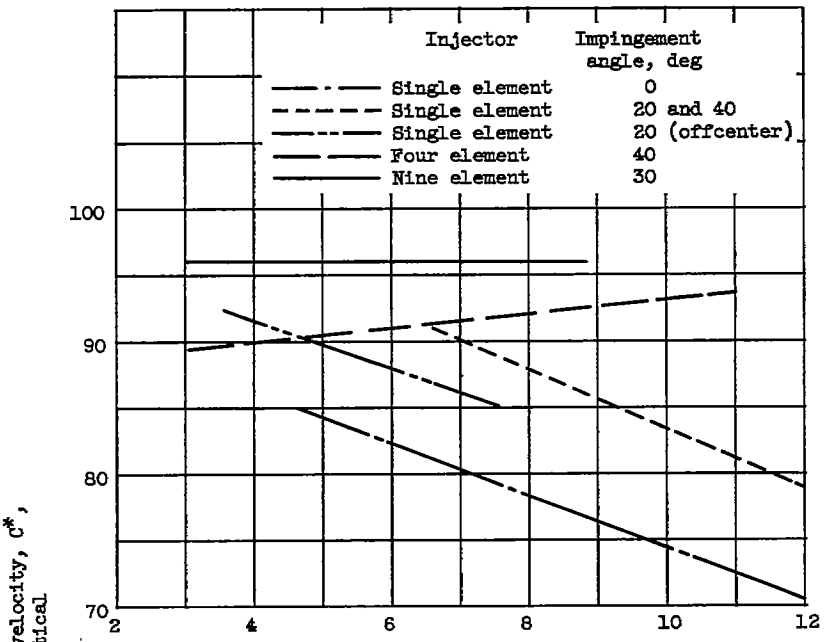

(a) Triplet injector in 12-inch chamber length.

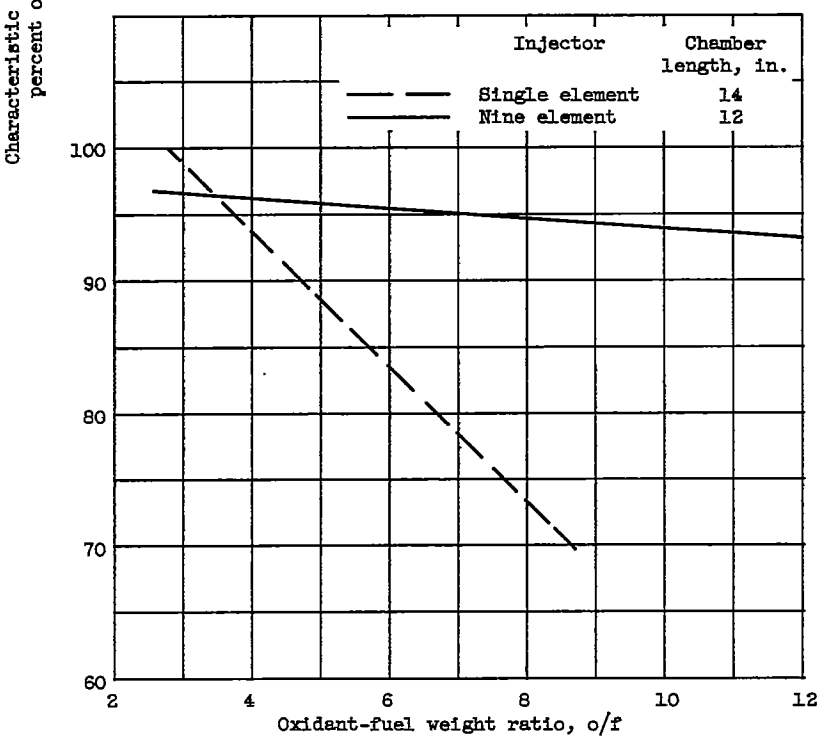

(b) Concentric-tube injector.

Figure 9. - Summary of injector performance.

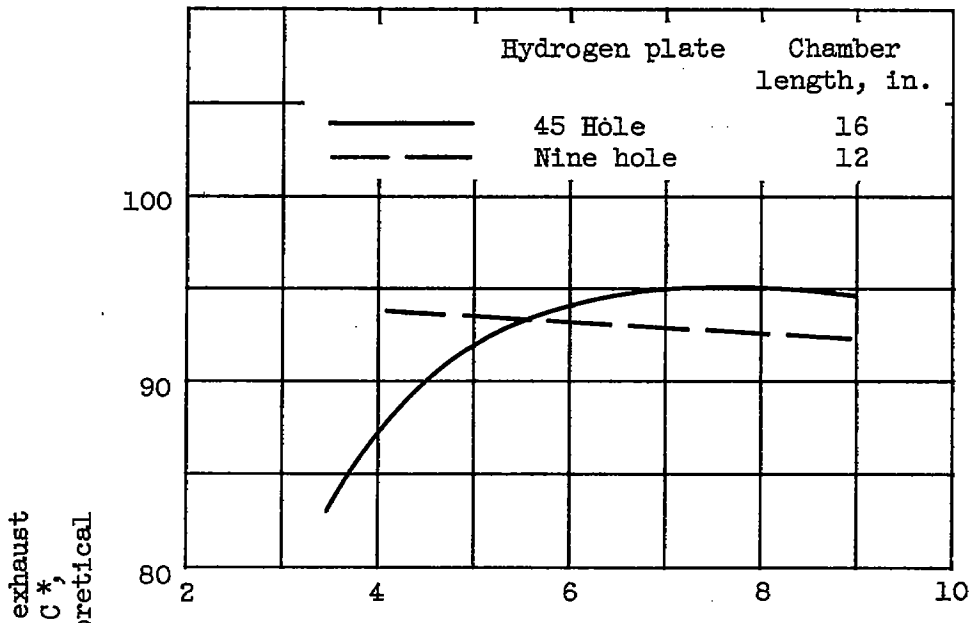

(c) Radial oxygen-jet injector.

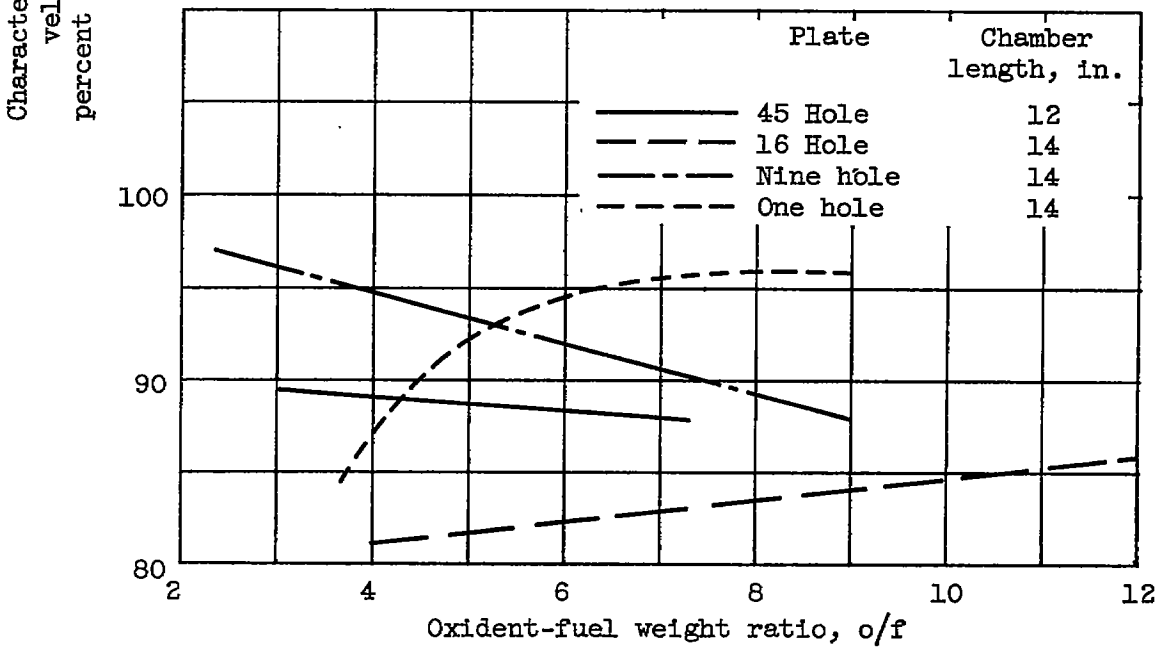

(d) Impinging oxygen-jet injector.

Figure 9. - Concluded. Summary of injector performance.

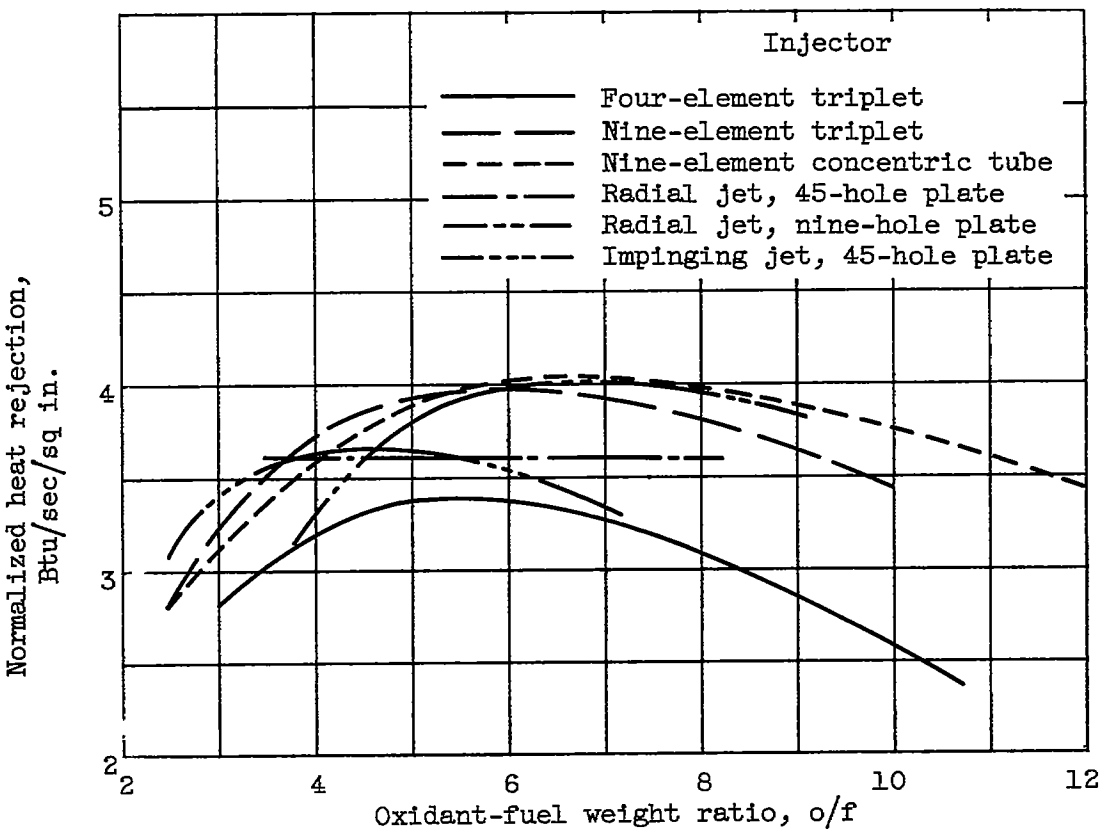

Figure 10. - Summary of heat rejection for various injectors.